UNIVERSITY OF TURKU

GO-BASED MEMBRANES FOR THE REMOVAL OF PHARMACEUTICALS FROM WASTEWATER

Materials Chemistry Research Group/ Materials Chemistry for Sustainable Development

Master's thesis

Chidimma Eberinwa

16.6.2026

Turku

Master's thesis

Subject: Materials Chemistry

Author: Chidimma Eberinwa

Title: GO Based Membranes for the Removal of Pharmaceuticals from Wastewater.

Supervisor(s): Prof. Carita Kvarnström, Joona Huopalainen

Number of pages: 50 pages

Date: 16.6.2026

Keywords: Graphene oxide (GO), Polyvinyl Alcohol (PVA), polyvinylidene fluoride (PVDF), Forward Osmosis (FO), Ultraviolet- Visible (UV-Vis) Spectroscopy.

Table of contents

Abstract

The increasing occurrence of pharmaceutical contaminants in wastewater has become a significant environmental concern due to their persistence and potential adverse effects on aquatic ecosystems and human health. The aim of this thesis, Graphene Oxide (GO)-Based Membranes for Removal of Pharmaceuticals from Wastewater, was to investigate the potential of graphene oxide-based membranes for the removal of selected pharmaceutical contaminants from aqueous solutions.

GO was synthesized from graphite flakes using a modified Hummers' method and GO membranes fabricated using the vacuum filtration technique onto a polyvinylidene fluoride (PVDF) support membrane. Self-standing GO/PVA composite membrane was also prepared to assess the influence of polymer incorporation on GO membrane modification, as well as its effect on the removal of pharmaceuticals residues and the membrane properties. The synthesized materials and fabricated membranes were characterized using UV–Visible spectroscopy, Raman spectroscopy, Fourier Transform Infrared Spectroscopy (FTIR), and X-ray Diffraction (XRD). Aqueous solutions of citalopram, diclofenac, amisulpride, carbamazepine, and metoprolol were filtered through the fabricated membranes using a syringe filtration system. The concentrations of the pharmaceuticals before and after filtration were determined using UV–Vis spectroscopy. In addition, forward osmosis (FO) experiments were conducted using GO/PVDF and GO/PVA membranes to evaluate water transport and reverse salt flux across the membranes.

The characterization results confirmed the successful synthesis of GO and the formation of GO-based membranes. Filtration experiments demonstrated that the GO/PVDF membrane selectively retained positively charged pharmaceuticals, while neutral and negatively charged pharmaceuticals exhibited lower retention. The incorporation of PVA altered the filtration behaviour of the pristine GO membrane and resulted in improved retention of neutral pharmaceutical compounds. FO experiments showed that the GO/PVA membrane exhibited enhanced water transport and lower reverse salt flux compared with the pristine GO/PVDF membrane, indicating improved membrane selectivity and structural stability due to the modification with PVA.

The study concludes that GO-based membranes are promising materials for the removal of pharmaceutical contaminants from wastewater. The membrane performance was strongly influenced by the physicochemical properties of the pharmaceutical compounds and the membrane composition. Furthermore, the incorporation of PVA improved membrane performance, especially in FO applications.

1 Introduction

Water pollution caused by chemicals has become a major concern and a priority for both society and public authorities. Water pollution happens when one or more substances are released into water, altering its natural state in a harmful way. These pollutants can create problems for humans, animals, their habitats, and the environment as a whole. Pharmaceutical compounds are classified as emerging contaminants and have been widely detected in various aquatic environments worldwide, including wastewater, groundwater, and drinking water sources.[1] Although pharmaceuticals provide significant benefits to human health, their widespread use and subsequent release into the environment pose serious risks to aquatic ecosystems and human health. Pharmaceuticals are designed to be resistant to biodegradation so that they remain stable until they have performed their intended pharmacological function after administration.[2] Many of these compounds are only partially metabolized and are excreted into water bodies through urine.[3] Due to their resistance to biodegradation, they persist and accumulate in aquatic systems with continuous releasele potentially causing toxic effects on marine organisms and disrupting ecological balance. The introduction of these pharmaceuticals and metabolites into aquatic environments, their accumulation in marine organisms through the food chain, and their eventual uptake by humans may lead to adverse effects.[4]

Conventional wastewater treatment consisting of a combination of physical, chemical and biological processes are not specifically designed to remove these micropollutants, leading to their persistence in surface waters, groundwater, and even drinking water sources. The presence of these compounds poses potential risks to aquatic ecosystems and human health, even at low concentrations.

To address this challenge, various advanced approaches have been explored for wastewater treatment, including the use of membrane-based technologies. In this study, GO-based membranes were investigated for their effectiveness in removing pharmaceutical contaminants from aqueous solution of the selected pharmaceuticals.

1.1 Graphene Oxide (GO)

GO consists of oxidized graphene sheets that originate from graphite and was previously referred to as graphite oxide or graphitic acid. It is produced through the chemical oxidation of graphite.[4–7] The oxidation of graphite has been investigated for more than a century, with the earliest reported preparation conducted by B.C. Brodie in 18594. Graphite is commonly treated with strong oxidizing agents, such as potassium permanganate ($KMnO_4$), in the presence of sulfuric acid, as first reported by Hummers'.[6]

GO nanosheets are a two-dimensional (2D)[7,8] nanomaterial with a thickness approximately equal to that of a single atomic layer. They are chemical derivatives of graphite and are rich in oxygen-containing functional groups, such as hydroxyl, epoxy, and carboxyl groups. GO contains both sp^2- and sp^3-hybridized carbon atoms. In the sp^2 regions, each carbon atom forms three strong σ-bonds with neighbouring carbon atoms, creating a planar network, while the fourth valence electron occupies a p-orbital, overlapping with neighbouring p-orbitals to form delocalized π-electrons above and below the plane. These π-electrons generate an electron-rich surface that is crucial for the chemical behaviour of GO, including the coordination of metal cations, stabilization of interlayer spacing, and tuning of membrane properties.

The basal planes of GO are primarily decorated with hydroxyl and epoxide groups, while the sheet edges are mainly occupied by carboxyl and carbonyl groups in a random manner, resulting in sheets with a mixed sp^2–sp^3 carbon framework.[9,10] While graphene consists of entirely ordered sp^2-bonded carbon, the structure of GO contains disordered sp^3-bonded carbon, introduced by oxygen functional groups, along with residual ordered sp^2-bonded carbon domains. GO can be readily dispersed in water due to the presence of a large number of oxygen-containing functional groups, which impart negative charges to the sheets, unlike pristine graphene. However, these functional groups disrupt the sp^2 carbon network, rendering GO electrically insulating, whereas graphene remains an excellent electrical conductor. To recover some of the desirable electrical, mechanical, and thermal properties of graphene, GO is typically reduced using thermal annealing or chemical reducing agents.[11–17] The resulting material, known as reduced graphene oxide (r-GO), exhibits improved conductivity; however, its electrical performance still

falls short of pristine graphene due to defects introduced in the graphitic structure during the reduction.

Figure 1 shows the synthesis of GO using modified Hummers' method. The process involves treatment with $NaNO_3$, H_2SO_4, $KMnO_4$, under ice bath, oxidation at room temperature with thermometer control and final addition of H_2O_2.

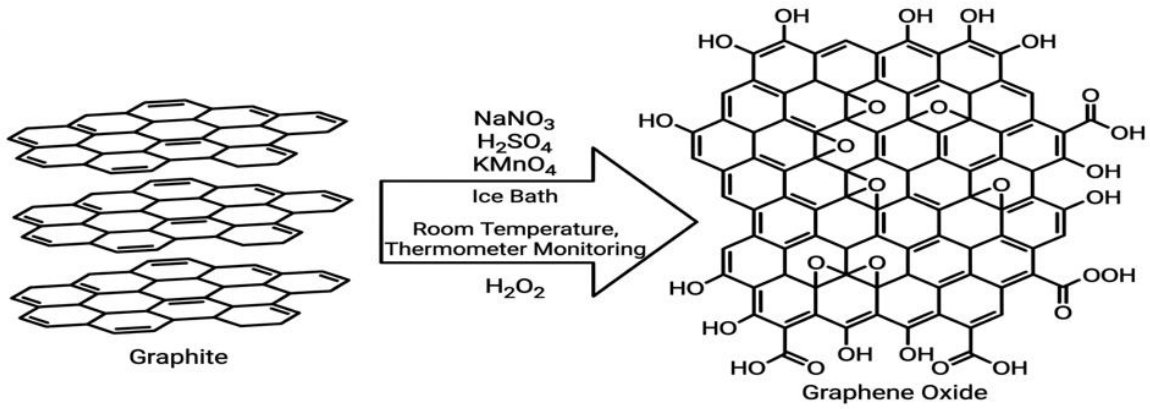

Figure 1: Graphical representation of the synthesis of GO from graphite via modified Hummers' method. Created by Figlabai.

1.2 GO Membranes

Over the past decade, GO membranes have attracted substantial scientific and technological attention due to their tunable microstructure, abundance of reactive functional groups, and exceptional water permeability, making them promising candidates for water purification applications.[18,19] The diverse chemical functionalities of GO sheets render them an adaptable platform for the fabrication of various graphene-based materials.

Membrane separation technologies have gained increasing attention as energy-efficient and reliable alternatives to traditional thermal separation methods. Unlike thermal processes, which require substantial energy input, membrane-based systems operate at lower energy costs while maintaining effective separation performance. Despite these advantages, widely used polymeric membranes are often limited by poor selectivity, vulnerability to fouling, and insufficient resistance to thermal and chemical degradation, which restricts their long-term use.

Consequently, there is ongoing interest in identifying and developing new membrane materials that combine high permeability with improved selectivity, fouling resistance, and chemical stability.[20] Carbon-based materials, including GO exhibit high thermal stability, strong mechanical properties, and excellent selectivity and permeability, making them attractive for membrane fabrication. GO membranes have attracted considerable attention due to their layered architecture and abundant oxygen functional groups, which enable high water flux and selective molecular transport. Their separation efficiency depends on the size, charge, and interactions of the permeating species with the membrane.[20] Water transport is proposed to occur either through oxidized regions that expand the interlayer spacing or through graphitic domains that provide low-resistance pathways for rapid flow.[21]

Membranes can be classified as dense and porous. Filtration mechanism based on porous membranes can be further classified as microfiltration (MF, pore size 0.1–10 μm), ultrafiltration (UF, pore size 0.001–0.1 μm), reverse osmosis (RO, pore size < 10 Å) and nanofiltration (NF, pore size 0.5–2.0 nm) membranes.[22] Porous membranes permit the passage of water while retaining particles based on their size, with pore sizes typically ranging from micrometres to nanometres. In contrast, dense membranes are non-porous solid structures, where separation is governed by the solubility and diffusivity of molecules rather than size exclusion. The commercial materials commonly used for membrane fabrication include polycarbonate (PC), polyvinylidene fluoride (PVDF), polyethersulfone (PES), polysulfone (PSF), polyamide (PA), and polyacrylonitrile (PAN).

GO membranes consist of graphene oxide nanosheets arranged in a layered structure. The interlayer spacing between adjacent sheets forms a network of nanocapillaries that serve as channels for water molecules to pass through.

Two types of GO membranes have received considerable attention due to their high water selectivity and permeability: ultrathin nanoporous GO membranes (also known as porous graphene)[23–30] and stacked-layer GO membranes containing two-dimensional water channels, including chemically modified and physically intercalated GO membranes.[21,31–36] The atomic thickness of nanoporous GO membrane is approximately one-third of a nanometer, which leads to significantly higher water permeability (6–66 $L \cdot cm^{-2} \cdot MPa^{-1}$) compared to thin-film composite

membranes (~0.24 $L \cdot cm^{-2} \cdot MPa^{-1}$), while still achieving nearly complete salt rejection (~100%).[37] Despite their excellent separation performance, the reliable fabrication of defect-free sub-nanometer pores (radius ~0.45 nm) in single-layer graphene remains technically challenging and difficult to scale up. Consequently, the practical application of nanoporous graphene membranes is still largely restricted to laboratory research.[38-40]

Stacked GO membranes with two-dimensional water channels have been extensively investigated, including both chemically treated and physically intercalated systems.[41] However, these membranes often exhibit microporous defects caused by improper stacking of graphene oxide laminates, commonly referred to as framework defects.[42,43] Such microporous defects act as non-selective transport pathways, thereby reducing water–solute selectivity in GO membranes.[43] The impact of these defects depends on the extent to which they are filled or minimized, with membranes containing fewer or smaller defects exhibiting improved separation performance. In addition to defect-related limitations, the structural stability of GO membranes remains a critical challenge, as GO nanosheets may undergo delamination or experience compaction of interlayer spacing under typical operating conditions, adversely affecting membrane performance over time. The self-assembly of GO nanosheets results in a lamellar membrane structure, where the interlayer spaces and tortuous pathways function as nanochannels for water and solutes. The architecture of these lamellae is influenced by the lateral size of the GO nanosheets as well as the presence of defects and wrinkles, which together govern both the water flux and the rejection of contaminants.[44]

1.3 Methods of GO Membrane Fabrication

Several techniques have been designed to prepare GO membranes. By employing these methods, GO nanosheets can be assembled into a layered, interconnected nano-capillary structure. These nano-capillaries, or nanochannels, function as selective barriers that permit rapid water permeation while effectively rejecting impurities and salt ions[45,46]. In these confined nanochannels, the unoxidized graphene domains provide low-friction transport pathways, resulting in enhanced slip of water molecules[47]. Consequently, the structure of the interlayer spacing plays a

critical role in determining the separation and purification performance of layered GO membranes.

However, GO membranes can be classified into two main types: supported membranes and self-standing membranes. Self-standing membranes are composed entirely of active material and, depending on their design and structure, can exhibit higher flow rates due to the absence of additional supporting layers. In contrast, supported membranes are often easier to fabricate, and by carefully selecting both the support material and the fabrication method, it is possible to achieve desirable combinations of mechanical, chemical, and transport properties.

1.3.1 Vacuum Filtration Technique

Vacuum filtration is a technique used to separate solids from liquids by creating a pressure difference across a membrane or filter paper, typically using a vacuum pump. The solid particles are retained on the filter surface, while the liquid passes through into a collection flask. In vacuum-assisted filtration, GO dispersions are filtered through a porous support, forming a membrane composed of stacked GO nanosheets retained on the substrate. It is a simpler, more cost-effective method for synthesizing graphene oxide membranes. However, this technique can produce membranes with a high density of defects, which often arise from the aggregation of graphene oxide sheets and uneven deposition of layers during the filtration process. In this work, vacuum filtration was employed to prepare the supported GO membranes, enabling uniform deposition of GO sheets on the membrane. A diagrammatic illustration of the fabrication of the membranes using this technique is presented in the Figure 2.

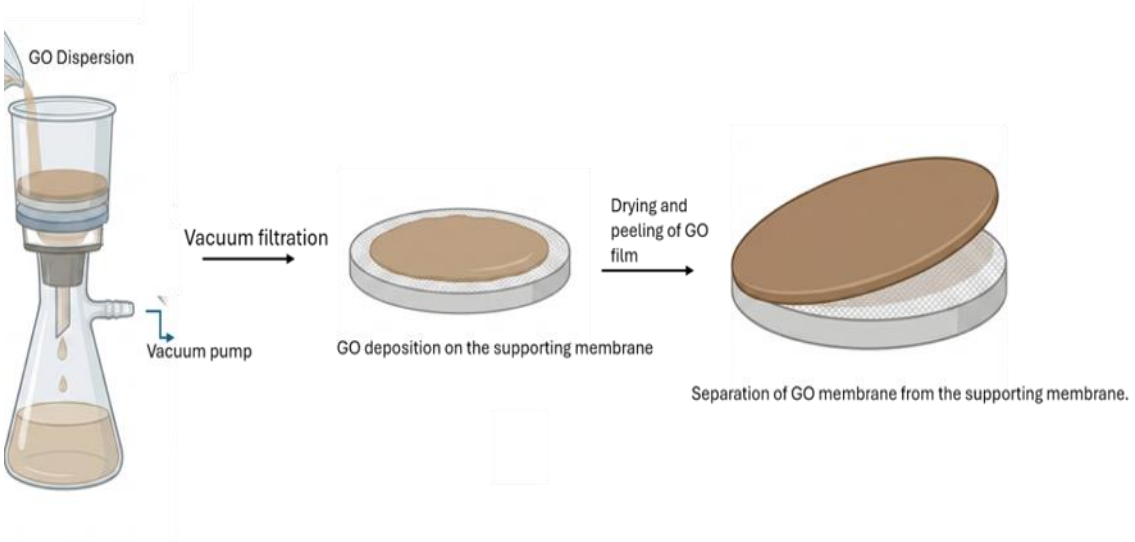

Figure 2: Schematic representation of the fabrication of the free-standing GO membrane by vacuum filtration using a porous polymer support. Created by figlabai.

1.3.2 Layer By Layer Assembly

Layer-by-layer (LbL) assembly is a thin-film fabrication technique in which a continuous membrane is built by sequentially stacking individual layers of material. In the case of GO membranes, the abundant oxygen-containing functional groups on GO sheets enable covalent bonding between layers, enhancing the membrane's stability in aqueous environments. By repeating the LbL process, membranes of controlled thickness can be produced, allowing precise tuning of structural and transport properties. However, the method is time-consuming, as each layer typically requires deposition, curing, and washing steps. Consequently, fabricating thick membranes through LbL assembly can be labour-intensive and less practical for large-scale applications.

1.3.3 Spin Coating

Spin coating is a rapid film fabrication technique often combined with heating to achieve the desired thin film within a short period. In this method, a small amount of GO solution is deposited onto a substrate, which is then rotated at high speed. The centrifugal force spreads the solution evenly across the surface, forming a uniform thin layer. By adjusting parameters such as spin speed, spin duration, and the concentration or volume of the GO solution, it is possible to precisely control the thickness, morphology, and uniformity of the resulting GO film.

1.3.4 Drop Casting

Drop casting is one of the simplest and most used techniques for the fabrication of GO membranes. In this method, a small volume of GO dispersion is deposited onto a flat substrate and allowed to spread across the surface. As the solvent evaporates, the GO sheets gradually assemble and stack, forming a layered membrane structure. However, this technique is considered one of the most basic approaches for producing GO films. During the deposition process, there are no significant surface-ordering or external driving forces to guide the arrangement of GO sheets. As a result, the sheets tend to deposit and stack in a relatively random orientation, making it difficult to achieve a well-aligned and compact structure. This lack of controlled alignment can lead to reduced structural uniformity and potentially lower membrane quality compared with membranes fabricated using more controlled deposition techniques.

1.3.5 Dip Coating

This is a simple and widely used technique for fabricating thin GO films. In this method, a substrate is immersed into a GO dispersion and then slowly withdrawn from the solution. As the substrate is removed, a thin layer of GO solution remains adhered to its surface, which subsequently dries to form a GO coating. The thickness of the deposited layer can be controlled by adjusting parameters such as the withdrawal speed of the substrate, the concentration of the GO dispersion, and the temperature during the drying process. Despite its simplicity and ease of implementation, dip coating may present challenges in achieving highly uniform GO sheet arrangements, as the method provides limited control over the alignment and organization of the nanosheets during film formation.

1.3.6 Pressure-Assisted Assembly

It is a technique for fabricating GO membranes in which positive pressure is applied to the GO dispersion, forcing the solution through a porous substrate. As the solvent passes through, the GO sheets are retained on the surface, forming a compact, layered membrane. This method promotes faster deposition and improved stacking of GO sheets, resulting in membranes with higher packing density, better uniformity, and enhanced mechanical stability. In comparison, vacuum filtration uses negative

pressure beneath the substrate to pull the solvent through, allowing GO sheets to accumulate gradually. While vacuum filtration is simple and widely used, it provides only moderate control over sheet alignment and layer compactness. When carefully controlled, pressure-assisted assembly generally produces higher-quality membranes than vacuum filtration, although vacuum filtration remains popular in laboratory settings due to its ease of use and minimal equipment requirements.

1.3.7 Spray Coating

It is a technique for fabricating GO membranes, in which the GO solution is sprayed onto a substrate as very fine droplets. As the solvent evaporates, the GO sheets remain on the surface, forming a thin and uniform layer. The thickness and morphology of the membrane can be controlled by adjusting factors such as droplet size, spray speed, solution concentration, and substrate temperature. Similar to dip coating, spray coating is relatively insensitive to the shape of the substrate, allowing uniform deposition on flat, curved, or irregular surfaces.

1.3.8 Bar/Doctor Blade Coating

Bar coating and doctor blade coating are among the most widely used scalable methods for fabricating GO membranes. Concentrated GO dispersions can exhibit viscoelastic behaviour due to hydrogen bonding between water molecules and the oxygen-containing functional groups on the GO sheets. During the coating process, a shear force is applied to the viscous gel, which helps align the GO laminates, producing a continuous and compact layered structure. This method allows the fabrication of high-quality membranes with thicknesses as low as approximately 100 nm, although it becomes challenging to prepare ultrathin films below 10 nm. A notable limitation of this approach is its sensitivity to the shape of the substrate, which must be flat and level to ensure uniform alignment of the GO sheets.

1.3.9 Slot-Die Coating

Slot-die coating is a scalable technique for fabricating GO membranes, in which a GO solution is pumped through a narrow slit (slot) onto a moving substrate. As the solution spreads, a thin wet layer is deposited, and the shear force generated between the moving substrate and the liquid meniscus aligns the GO sheets, forming

a well-ordered, laminar structure. A key advantage of this method is that it allows the use of low viscosity GO dispersions, which are relatively thin, watery solutions with lower GO concentrations. These dispersions can be applied directly without extensive pretreatment, enabling the production of ultrathin, uniform membranes. The thin wet layer also dries rapidly, reducing overall fabrication time, while the direct coating onto the substrate ensures minimal material waste. Additionally, slot-die coating can be adapted for different membrane materials or composite systems, making it a highly controllable, efficient, and scalable approach for producing high-quality GO membranes.

1.4 Membrane-Based Water Filtration Techniques

This is a widely employed separation technique across various industries, used to remove particles, microorganisms, and solutes from liquids such as solutions or wastewater. This process utilizes semi-permeable membranes that selectively allow certain substances to pass while retaining others based on size or chemical properties. Membrane filtration is a key technology in both chemical processing and water treatment, providing reliable and efficient performance with minimal chemical input. Usually, chemical techniques are employed as a pretreatment step prior to membrane filtration.

Membrane-based technologies are widely used for the purification of pharmaceutical solutions. These methods can be classified into pressure-driven membrane processes (PDMPs), including microfiltration (MF), ultrafiltration (UF), nanofiltration (NF), and reverse osmosis (RO), and osmotically driven membrane processes (ODMPs), such as forward osmosis (FO) and pressure-retarded osmosis (PRO). PDMPs use hydraulic pressure to push water through a semi-permeable membrane, while ODMPs rely on osmotic pressure differences between the feed and draw solutions to drive water transport. In both cases, contaminants are primarily separated based on their size or molecular properties.

1.4.1 Microfiltration (MF)

This is widely used to remove suspended particles and colloidal matter from solutions. Acting like a fine sieve, MF employs a semi-permeable membrane with pore sizes typically ranging from 0.1 to 10 μm, through which pressure drives the

liquid, retaining larger particles while allowing the solution to pass. The membranes are relatively thick, often between 10 and 150 μm[48], to provide mechanical strength and durability under pressure. MF membranes have been reported to be fairly efficient at removing colloidal and particulate matter, retaining approximately 40% of organic compounds.[49] Its modules are typically manufactured from materials such as high-density polyethylene, glass fiber-reinforced plastic, polypropylene, polycarbonate, or ceramics. In specific applications that require the removal of smaller particles, ceramic MF membranes are often preferred.

1.4.2 Ultrafiltration (UF)

Ultrafiltration operates in the size range between microfiltration and nanofiltration, with pore sizes typically ranging from 0.001 to 0.1 μm. While the filtration mechanism is similar to that of MF, UF membranes provide higher water clarity and safety, as they are capable of removing viruses, bacteria, colloids, and suspended particles. UF finds applications in drinking water purification, wastewater treatment, and biopharmaceutical processing, where the removal of smaller contaminants is essential for quality and safety. Common materials for ultrafiltration (UF) membranes include polymers such as polysulfone (PS), polyethersulfone (PES). These polymeric membranes offer excellent mechanical strength, chemical resistance, and thermal stability, while enabling precise control over pore size, which is essential for selective separation of contaminants in water and wastewater treatment.

1.4.3 Reverse Osmosis (R0)

RO is a widely used water purification technique that employs a semi-permeable membrane to remove dissolved salts, organic compounds, and other impurities. It has gained significant interest in water treatment because of its ability to produce high volumes of purified water efficiently.

It allows water molecules to pass through while rejecting ions and dissolved organics, producing purified water suitable for drinking, irrigation, and industrial applications. RO membranes are commonly made from polyamide or cellulose acetate, with variations including barrier and nanofiltration membranes designed for specific applications. RO has been applied in treating industrial effluents, such as those from the petrochemical, chemical, and food processing industries, as well as in

the removal of pesticides, plastic additives, and pharmaceutically active compounds. Its main advantages are the production of high-quality water and removal of a broad range of contaminants, while the disadvantages include high energy requirements, membrane fouling, and maintenance costs.

1.4.4 Forward Osmosis (FO)

It is an ODMPs which uses membrane- based technology for water treatment. FO is a membrane-based separation process driven by osmotic pressure differences between a low-salinity feed solution and a high-salinity draw solution. Water naturally moves from the feed solution to the draw solution across a semi-permeable membrane, while most dissolved solutes and ions in the feed solution are retained. As water transfers, the draw solution becomes diluted, reducing its osmotic pressure, while the feed solution becomes slightly more concentrated, causing a small increase in its osmotic pressure. This process continues until the net driving force for water movement becomes negligible, a state often referred to as osmotic equilibrium. At this point, water transport essentially stops, even though the draw solution remains more concentrated than the feed solution. Because the diluted draw solution cannot be used directly as freshwater, an additional separation step is required to remove the draw solutes and recover potable water.

The FO process is schematically illustrated in Figure 3. In this study, the FO technique was applied using both GO/PVDF and GO/PVA membranes as the active separation membranes while, sodium chloride (NaCl) solution was used as the draw solution.

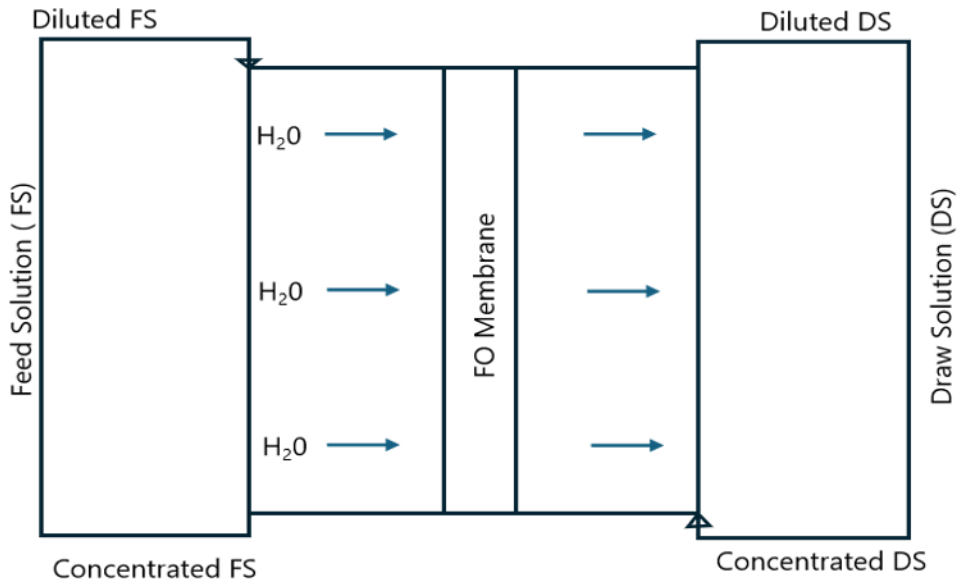

Figure 3: Schematic Illustration of Forward Osmosis

1.4.5 Pressure Retarded Osmosis (PRO)

Most water purification processes are energy intensive. In contrast, PRO utilizes the salinity gradient between two water bodies to generate energy. PRO is a membrane-based process similar to FO; however, it enables the production of sustainable osmotic power. In PRO, hydraulic pressure is applied on the draw solution side, creating a chemical potential difference between seawater and freshwater while allowing controlled water flux. This flux can be converted into mechanical energy and subsequently into electricity, with water transport occurring in the same direction as in FO. Nevertheless, membrane fouling remains a significant limitation, as it reduces permeate flux and osmotic power generation, thereby increasing overall operational costs, similar to other membrane-based technologies.

Membrane technology has become an essential tool across many industrial sectors, including the food, pharmaceutical, textile, petrochemical, chemical, lithium-ion battery, fuel cell, gas separation, and water and wastewater treatment industries. Membrane-based technologies provide cost-effective solutions with high contaminant removal efficiency, relatively low energy consumption, and widely available raw materials. Over the past two decades, synthetic membranes have largely replaced cellulose-based membranes such as cellulose diacetate, cellulose triacetate, and regenerated cellulose due to their higher resistance to harsh operating conditions[50-52]. Synthetic membranes can be manufactured from either organic materials

(polymers) or inorganic materials such as metals, metal oxides, and ceramics. Membrane fabrication therefore offers considerable flexibility, as various materials can be used, including ceramic materials (e.g., zirconia, titania, silica, and alumina), metals (e.g., silver, palladium, and copper), and polymers such as polyvinylidene difluoride (PVDF), polyethersulfone (PES), polysulfone (PSF), polyvinyl alcohol (PVA), polytetrafluoroethylene (PTFE), polypropylene (PP), polyamide (PA), polyimide, poly(1-vinylpyrrolidone) (PVP), polyvinyl chloride (PVC), and polyacrylonitrile (PAN).

They are essential components widely employed in filtration systems across various industries. The selection of membrane material significantly influences filtration performance, including separation efficiency and flow characteristics, as well as factors such as chemical stability, fouling resistance, and overall operational durability.

1.5 Polymeric Membranes Materials

1.5.1 Polyvinylidene Fluoride (PVDF) Membranes

PVDF membranes are generally hydrophobic microporous membranes. PVDF is a highly non-reactive thermoplastic fluoropolymer with the repeating unit $(C_2 H_2 F_2)_n$. It is semi-crystalline, mechanically strong, and flexible, which makes it suitable for membrane fabrication. PVDF serves as a key material for the fabrication of both UF and NF membranes.

PVDF is one of the most used membrane materials. It can achieve salt rejection and highly effective for water purification and various industrial separation processes.

In this research, a PVDF/GO membrane was employed for the removal of pharmaceuticals from aqueous solutions.

1.6 Regulation of GO Membranes

The interaction of water molecules with GO layers can alter the stacked structure of the flakes, which may reduce the mechanical stability of the membrane. This occurs because water molecules become trapped between the GO layers, leading to the expansion of membrane channels. The resulting swelling weakens the hydrogen

bonding between adjacent GO flakes, further decreasing the structural stability of the membrane. GO membranes typically exhibit an interlayer spacing of approximately 9 Å in the dry state. However, when exposed to water, their hydrophilic nature causes the interlayer distance to expand to values of up to about 13 Å.[53-55]

The stability of GO flakes in aqueous environments is strongly determined by the type, distribution, and chemical behaviour of oxygen-containing functional groups on their surfaces. Functional groups such as hydroxyl (–OH), epoxy (–O–), and carboxyl (–COOH) facilitate intermolecular interactions between neighbouring GO sheets. Hydroxyl groups play a significant role in stabilizing the layered structure by forming hydrogen bonds with oxygen-containing groups on adjacent flakes, thereby strengthening interlayer cohesion and helping maintain membrane integrity. Conversely, carboxyl groups exhibit different behaviour in aqueous systems, as they can undergo hydrolysis and become deprotonated depending on the pH of the environment. As a result, their ability to participate in hydrogen bonding is most effective when they remain protonated under acidic conditions, where they can contribute to interlayer hydrogen bonding and structural stability.[56-57]

1.6.1 Co-Ordination of Graphene Oxide with Metal Cations

This involves the chemical coordination of GO with metal cations, such as Ag^{+}, Cu^{2+}, Fe^{2+}, Fe^{3+}, and Mn^{2+}, through its oxygen-containing functional groups (hydroxyl, epoxy, and carboxyl) to enhance the stability of GO membrane. One of the primary limitations of graphene oxide membranes is the deterioration of their stability over prolonged use.[58]

The oxygen-containing functional groups on both the basal plane and edges of GO enable it to disperse in water and organic solvents, providing extensive possibilities for designing materials based on GO. GO membranes with nanostructured architecture are typically formed by the stacking of graphene oxide sheets with lateral dimensions of approximately 1–10 μm. The interlayer spacing between these sheets generally ranges from 0.9 to 1.2 nm, which is attributed to the presence of oxygen-containing functional groups such as epoxide, hydroxyl, and carboxyl groups.[59] Because these functional groups are distributed irregularly across the GO surface, interconnected pathways of unoxidized graphene domains can form, creating

channels that enable mass transport through the membrane structure.[60] Despite these advantages, GO membranes fabricated at the laboratory scale often lack the physicochemical robustness and mechanical strength required for large-scale industrial applications. To improve their structural stability and rigidity, researchers have introduced multivalent metal cations that act as cross-linking agents between adjacent GO nanosheets, thereby strengthening the membrane framework.[61-63]

Considerable research has therefore focused on enhancing the stability of GO membranes through various modification strategies. One approach involves the partial removal of oxygen-containing functional groups from GO nanosheets via thermal or chemical reduction, which can significantly alter their physicochemical properties.[64-68] Another simple and effective strategy is the intercalation of multivalent metal cations derived from metal salts. Metal ions such as Cu^{2+}, Fe^{2+}/Fe^{3+}, Ni^{2+}, Zn^{2+}, Ca^{2+}, Mn^{2+}, Mg^{2+}, and Al^{3+} can intercalate between GO sheets and promote interlayer crosslinking, thereby improving the membrane's resistance to swelling in aqueous environments.

Metal ions can form coordination complexes with oxygen-containing functional groups, stabilizing the interlayers through cation–π and electrostatic interactions.[69] Multivalent metal cations intercalate between GO sheets through electrostatic attraction and coordination bonding with oxygen-containing functional groups, forming ionic crosslinks. These crosslinks reduce electrostatic repulsion between layers, suppress swelling in aqueous environments, and enhance mechanical and structural stability.

1.6.2 Intercalation with Polymers

Cross-linking agents can intercalate within GO layers, allowing the interlayer spacing to be adjusted, optimizing the mass transfer channels of the membrane, and enhancing its water flux. They also serve as linkers that anchor the GO sheets, helping to stabilize the overall structure of GO membranes. Polyvinyl alcohol (PVA), rich in hydroxyl groups, can easily form a cross-linked mesh, offer good biocompatibility, and maintain stable physicochemical properties. Polyethyleneimine (PEI) is widely used to control the interlayer structure of GO membranes due to its

abundant amino groups, strong hydrophilicity, and high positive charge; its long-chain structure enables it to simultaneously connect and stabilize multiple GO nanosheets.

This study also investigates the intercalation of PVA into GO membranes to further enhance their structural stability.

2 MATERIALS AND METHODS

Table 1 Materials employed during the experimental methods.

Name of the material	Manufacturer
Sulfuric acid (H_2SO_4, ≥ 95%)	Sigma Aldrich
Potassium Permanganate ($KMnO_4$)	Sigma Aldrich
Hydrogen Peroxide (H_2O_2, 30%)	Sigma Aldrich
Sodium Nitrate ($NaNO_3$)	Sigma Aldrich
Polyvinyl Alcohol (PVA)	Sigma Aldrich
Sodium Chloride (NaCl)	Sigma Aldrich

2.1 Synthesis Of GO Using Modified Hummers' Method

An experimental setup was assembled with a three-neck bottle placed in an ice bath. Graphite flakes (2.0 g) were mixed with sodium nitrate (1.5 g) in the three-neck bottle firstly. Slowly, 125 ml of $H_2\ SO_4$ was added to the above mixture while stirring, which formed a black suspension.

$KMnO_4$ (9.0 g) was then added gradually to the suspension, and the mixture was allowed to react for two hours in the ice bath. The colour was changed to a dark purple-brown mixture at the end of the reaction.

Next, the reaction mixture was slowly allowed to warm up to room temperature. The temperature was continuously monitored using a mercury thermometer inserted into one end of the three-neck flask, thereby, maintaining it at which ensured it at room temperature. The reaction mixture was stirred continuously at 750 rpm in a cold-water bath for six days and the colour transitioned to a yellowish-brown with viscous suspension appearance. 6 ml of 30% H_2O_2 was slowly added to consume any remaining $KMnO_4$ and complete the oxidation process. The mixture was then stirred, which produced a yellowish-brown solution.

The GO solution formed was highly acidic (pH 1) because of the presence of sulfuric acid. Therefore, the solution was washed and centrifuged severally using an Heraeus Biofuge stratos centrifuge. During this process, the appearance of GO changed into a sticky, syrup-like liquid. The pH also increased to 4. After the washing process, the

GO solution was adjusted to 400 mL with deionised water, which resulted in a final concentration of 5 mg/mL.

2.2 Membrane Fabrication

A volume of 2 µL of the GO dispersion was diluted with 4.998 mL of DI water to prepare 5 mL of GO solution (0.002 mg/mL), corresponding to a total GO mass of 0.01 mg. The solution was gently mixed to ensure homogeneity. The diluted GO solution was deposited onto a hydrophilic PVDF Durapore membrane (47 mm diameter, 0.22 µm pore size) using a vacuum filtration setup (Figure 4). The membrane was carefully placed on a glass frit membrane support, with its reflective surface serving as the active site for GO deposition. The GO solution was poured into the funnel and filtered under reduced pressure, resulting in uniform deposition on the membrane surface. After filtration, the membrane was placed in a desiccator for complete drying. A brownish homogeneous GO layer was observed on the membrane surface which formed the GO/PVDF membrane.

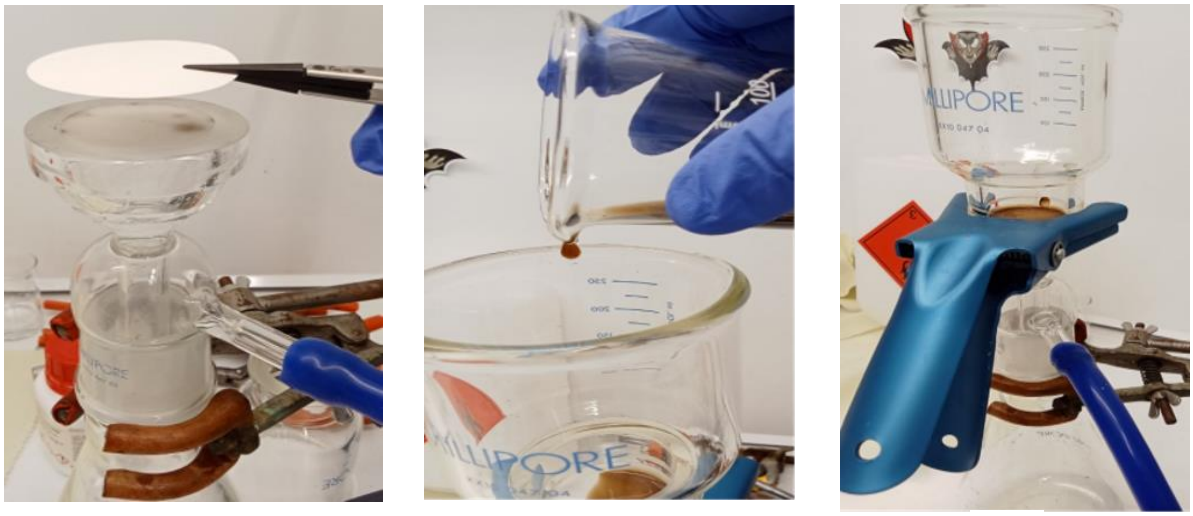

Figure 4: Membrane fabrication procedures. (A) Placement of the PVDF Membrane (B) GO Deposition of the Membrane (C) Filtration set-up with GO deposition on the membrane.

In addition, GO/PVA membrane was fabricated by dissolving 1 mg of PVA in 8.2 mL of deionized water under continuous stirring at 500 rpm and heating at 80 °C for 1

hour until a clear solution was obtained. The PVA solution was subsequently added to a GO dispersion containing 9 mg of GO (1.8 mL GO dispersed in 8.2 mL deionized water). The resulting PVA/GO mixture was further stirred at 500 rpm for approximately 15 minutes to ensure homogeneity. The PVA/GO membrane was then fabricated using a vacuum filtration technique, onto a PVDF support membrane. After filtration, the formed membrane was placed in a desiccator and allowed to dry, then carefully detached from the PVDF support to obtain a self-standing GO/PVA-based membrane.

2.3 Materials Characterization

A self-standing GO membrane was fabricated from 0.025 mg of GO following the same procedure used for the GO/PVDF membrane. After drying, the membrane was carefully detached and used for characterization. However, the mass of the GO/PVA membrane was maintained at 10 mg.

2.3.1 Raman Characterization

Raman spectra of the materials were obtained on a Renishaw invia Qontor Raman spectrophotometer. A 532 nm laser was used as the excitation source with a 20× objective lens, and a laser power of 0.5 %. The samples were placed on a Si substrate prior to measurement.

2.3.2 UV-Vis Characterization

UV–Vis spectroscopy was employed to analyse the optical properties of GO. Measurements were performed using an Agilent Cary 60 UV–Vis spectrophotometer over the wavelength range of 190–800 nm. 0.002 mg/mL of GO solution in a total volume of 5 mL were prepared and placed in a quartz cuvette with a 1 cm path length for spectral acquisition. Absorbance spectrum was obtained.

Aqueous solutions of pharmaceuticals were also analysed using UV–Vis spectroscopy before and after filtering them through fabricated GO/PVDF and GO/PVA membranes. Analysis of the pharmaceutical concentrations was based on the Beer–Lambert law: $A = \varepsilon cl$, where A is the absorbance, ε is the molar absorption coefficient ($L \cdot mol^{-1} \cdot cm^{-1}$), C is the concentration of the analyte ($mol \cdot L^{-1}$), and l is the path length of the cuvette (cm).[70]

2.3.3 XRD Characterization

The self-standing GO and GO/PVA membranes as well as the graphite flakes were characterized using Malvern Panalytical Aeris X-ray diffraction (XRD) diffractometer equipped with Cu Kα radiation source to investigate their crystalline structure and interlayer spacing calculated using the Bragg's equation, $n\lambda = 2d \sin\theta$, where n is the diffraction order (n =1 is first order, n =2 is second order [71], n = 3 is third order [72], λ is the wavelength of incident X-rays, d is the interlayer spacing between the crystal lattice planes and θ is the angle of incidence (glancing angle).

2.3.4 FTIR Characterization

The FTIR spectra of the self-standing membranes (GO and GO/PVA) were measured using Bruker VERTEX 70 spectrometer combined with Harrick Scientific Products' VideoMVP Single Reflection ATR Microsampler and a diamond ATR crystal. A small piece of the self standing GO membrane was placed on the IR crystal, and the IR characterization was performed at an ATR pressure of 83. The same procedure was repeated for the GO/PVA material.

2.4 Filtration Experiment

2.4.1 Syringe Filter

A circular piece of the membrane intended for pharmaceuticals filtration was cut and fitted into a syringe filter holder. The holder was then connected to a syringe pump. For each filtration experiment, a separate injection syringe containing the specific pharmaceutical solution was attached to the filter holder housing the membrane. The system was linked to software that enables controlled injection of the aqueous solution of the pharmaceuticals and the water flux through the membrane. The syringe filtration set is shown in Figure 5.

2.4.1.1 With GO/PVDF Membrane

Aqueous solutions of pharmaceuticals—diclofenac, citalopram, metoprolol, carbamazepine, and amisulpride—were introduced individually using their respective injection syringes through the GO/PVDF membrane fitted into the syringe holder.

2.4.1.2 With GO/PVA Membrane

In the same way, aqueous solutions of pharmaceuticals—diclofenac, citalopram, carbamazepine, were introduced individually using their respective injection syringes and filtered through the GO/PVA membrane.

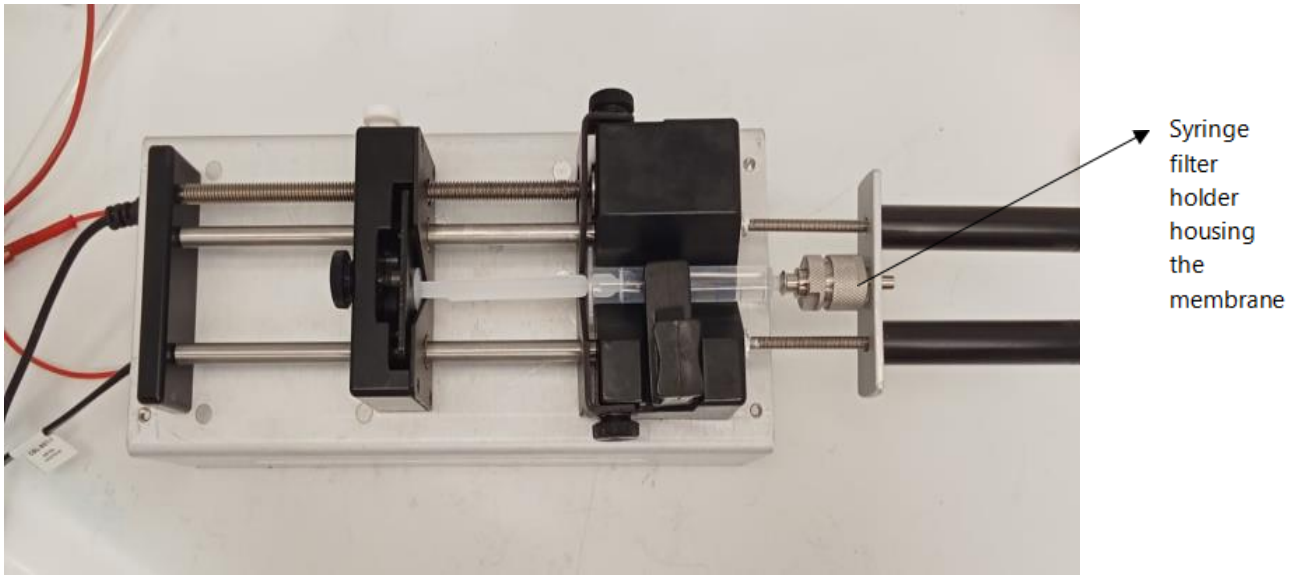

Figure 5: Syringe filtration set-up for the selected pharmaceuticals.

2.5 Forward Osmosis

5840 mg of NaCl was dissolved in 100 mL of DI water to obtain a 1 M solution making the draw solution for the experiment. Figure 6 depicts a GO/PVA membrane detached from its support. The GO/PVA and GO/PVDF membranes were separately used as the active separation membranes in the FO process. A volume of 40 mL of the draw solution and 100 mL of the feed solution was used. The process was allowed to run for 2 hours, during which the volume increase of the draw solution and the conductivity of the feed solution were measured at 15-minute intervals. An Orion conductivity meter was used to determine the electrical conductivity of the feed solution. Conductivity is governed by the presence of dissolved ionic species in the solution. The measured conductivity was used as an indicator of changes in salt

concentration during the FO experiments.

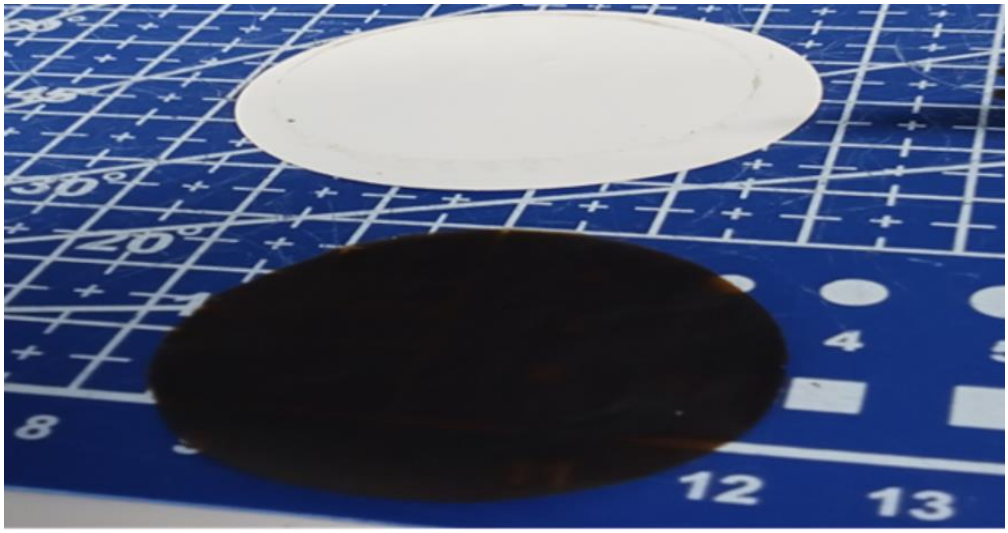

Figure 6: Self standing GO/PVA membrane obtained by detaching the membrane from the PVDF support.

3 RESULTS AND DISCUSSION

3.1 UV-Vis Characterization

The UV–Vis spectrum of GO dispersions shown in Figure 7 exhibits a characteristic absorption peak at approximately 230–235 nm. This peak is attributed to π→π* electronic transitions of the aromatic C-C bonds within the GO structure.[73] These C=C bonds are a prominent feature of GO, and this absorption band is commonly considered a defining spectral signature of the material.

A weak shoulder was observed around 300 nm. This corresponds to n→π* transitions of the C=O bonds [74,75] introduced during the oxidation of graphite to form GO. Although less intense than the primary peak, this feature is important for confirming the presence of oxygen-containing functional groups in GO. Together, these spectral features serve as diagnostic markers for the identification and quality assessment of GO dispersions.

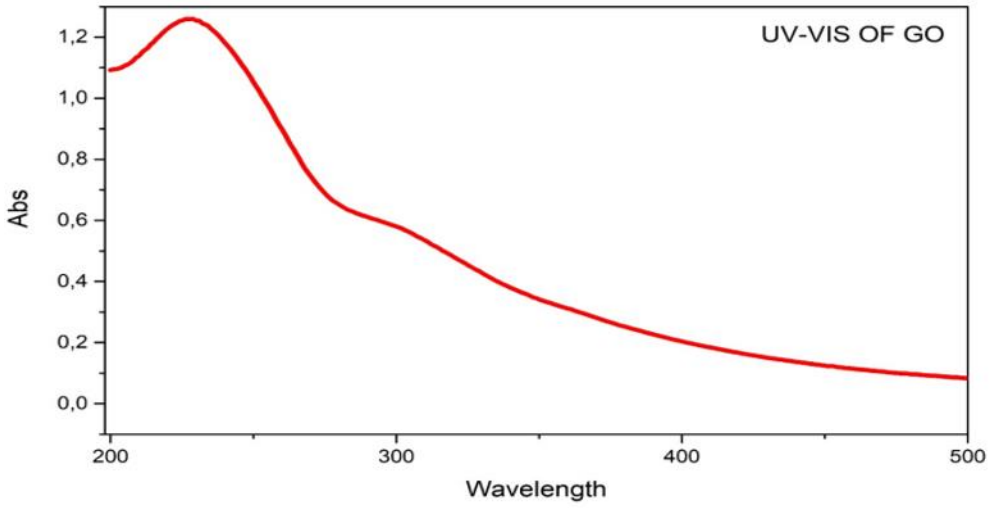

Figure 7: UV–Vis Spectrum of GO.

3.2 Raman Characterization of the Materials

The Raman spectrum of graphite presented in Figure 8 shows a strong and sharp G band at ≈1580cm^{-1}, corresponding to the in-plane vibration of sp²-bonded carbon atoms which arises from the first-order scattering of the E_2 g phonon mode.[76] A prominent 2D band was observed near 2700 cm^{-1} which confirmed the multilayer graphitic structure. The D band around 1350 cm^{-1} was weak or nearly absent which revealed a low defect density and high crystallinity of the graphite material.

Comparably, in Figure 9, the GO dispersion exhibits two main characteristics peaks of GO: the prominent D band at ≈1360 cm^{-1} and the G band at around 1590 cm^{-1}. The D band "becomes prominent, indicating the reduction in size of the in-plane sp^2 domains, possibly due to the extensive oxidation".[77] The D band arises from breathing modes of sp^2 carbon rings and is associated with structural defects, edges, and disorder within the GO lattice. A Si peak of 520 cm^{-1} was also observed.

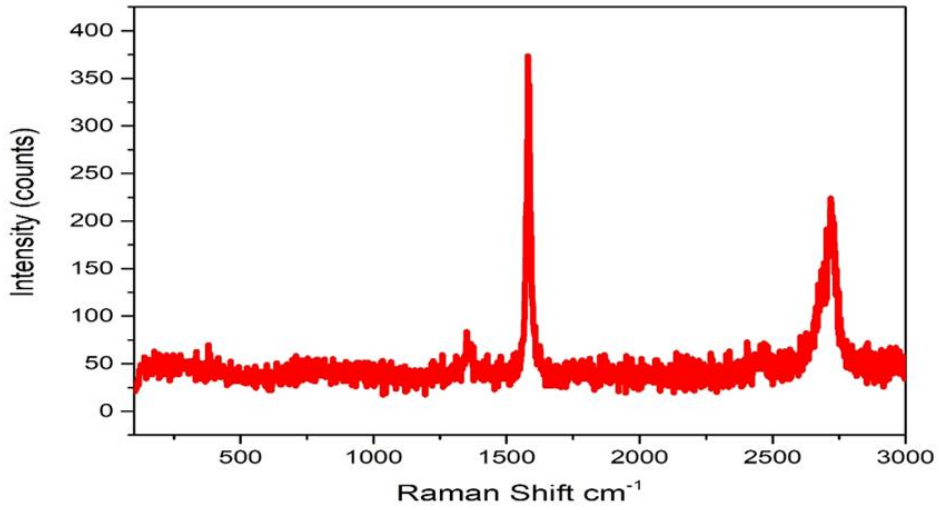

Figure 8: Raman Spectrum of graphite.

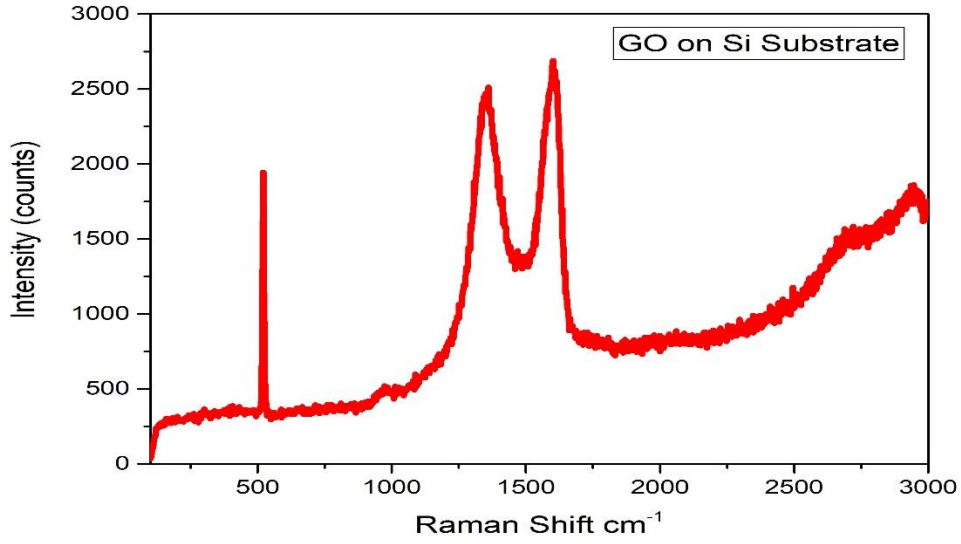

Figure 9: Raman Spectrum of GO.

The ratio of the D and G band intensities (I_D/I_G) is commonly used as a measure of the degree of disorder and defect density in graphitic materials, and it serves as an important parameter for characterizing structural defects in graphene-based

systems.[78-80] Thus, the Raman spectrum of GO exhibits a higher I_D/I_G ratio compared to pristine graphite due to the introduction of defects and functional groups during the oxidation process.

The Raman spectrum of PVA displayed in Figure 10 depicts a characteristic peak at ≈2900 cm^{-1}, which was attributed to the C-H stretching in PVA.[81] A weak non-prominent peak observed near 1490 cm^{-1} was assigned to O–H bending vibrations in PVA.

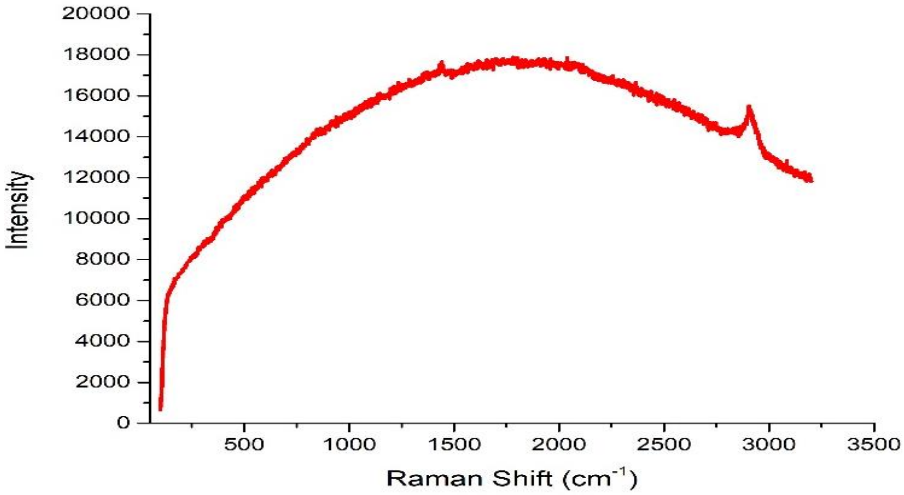

Figure 10: Raman Spectrum of Polyvinyl Alcohol.

In Figure 11, the Raman spectra of GO and GO/PVA membranes showed the characteristics D (≈ 1400 cm^{-1}) and G (≈1700 cm^{-1}) bands which are visible peaks in the GO Raman spectrum. The absence of the characteristic PVA peak (≈2900 cm^{-1}) in the GO/PVA peak could be attributed to the doping thus making the peak susceptible to defects arising from the interactions between the two molecules.

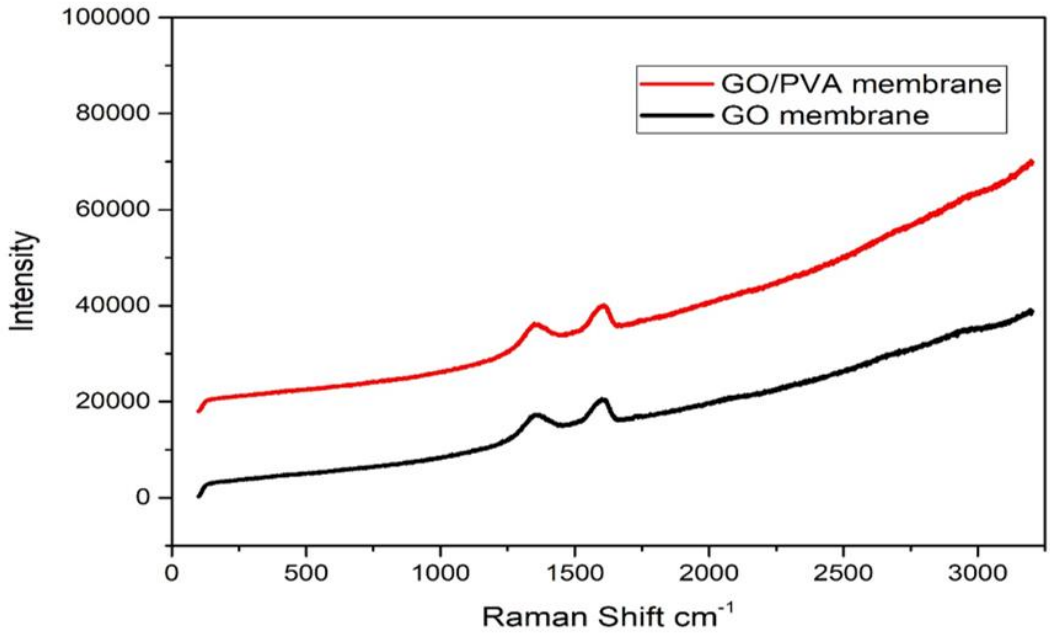

Figure 11: Raman spectra of GO and GO/PVA membrane.

3.3 FTIR Characterizations of the Membranes

The FTIR spectrum of GO membrane in Figure 12 confirms the presence of the oxygen containing functional group in the GO skeleton. The broad absorption band around 3200–3600 cm^{-1} was attributed to O–H stretching vibrations of hydroxyl groups. The bands observed at approximately 1720, 1600, and 1300 cm^{-1} were assigned to C=O stretching vibrations, skeletal vibrations of sp^2-hybridized C=C bonds in graphitic domains, and O–H bending vibrations, respectively.[82]

Likewise, the FTIR spectrum of the GO/PVA membrane was dominated by characteristic GO absorption bands, including O–H stretching (≈3200–3500 cm^{-1}), C=O stretching (≈1720 cm^{-1}), and C–O vibration (1300 cm^{-1}). However, changes were observed within the 1000–1500 cm^{-1} region of the membrane. Particularly, peak shoulders near 1250 and 1300 cm^{-1} were evident in the GO/PVA membrane. These features are consistent with C-H wagging vibrations associated with the incorporation of PVA into the GO matrix.

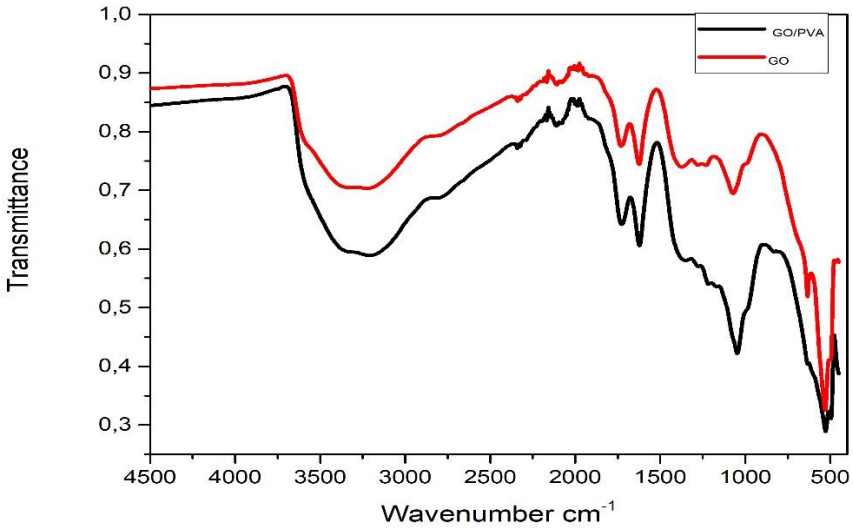

Figure 12: FTIR spectra of GO and GO/PVA membrane.

3.4 XRD Characterization of the Membranes

The XRD pattern of pure graphite in Figure 13, exhibits a sharp and intense diffraction peak at approximately 2θ = 27.0° which was assigned to the (002) plane of graphite with a d-spacing of 3.2 Å and a slight diffraction peak observed near 54.5°. The sharpness and high intensity of the diffraction peaks confirm the high crystallinity and layered structure of graphite. In Figure 14, XRD patterns of GO and GO/PVA membranes. The GO membrane showed an observed characteristic peak at ≈ 2θ = 11.0°, corresponding to the (001) plane and a d-spacing of 8.0 Å. In contrast, the GO/PVA composite membrane, exhibited a slight shift toward a lower 2θ values at ≈10.8 also assigned to the (001) plane which indicated slight increase in the d-spacing to ≈8.2 Å. The results demonstrate the successful synthesis of the GO and GO/PVA membranes, with the shift of the characteristic graphite peak, suggesting an increase in interlayer spacing.

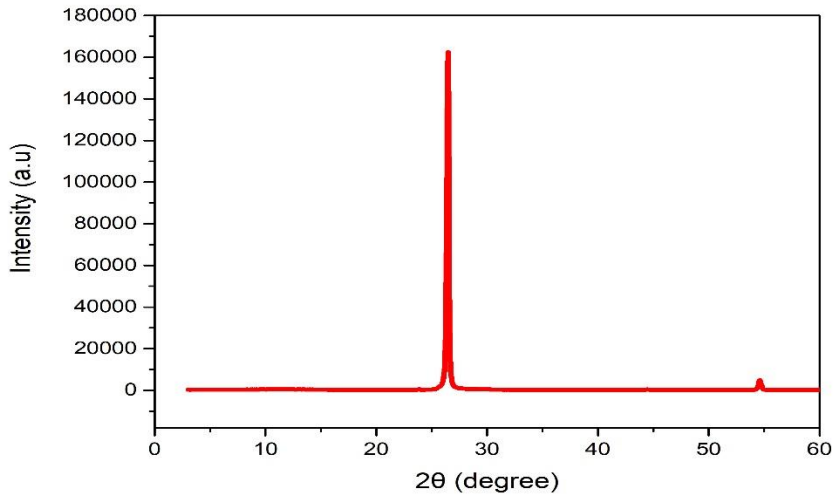

Figure 13: XRD pattern of graphite.

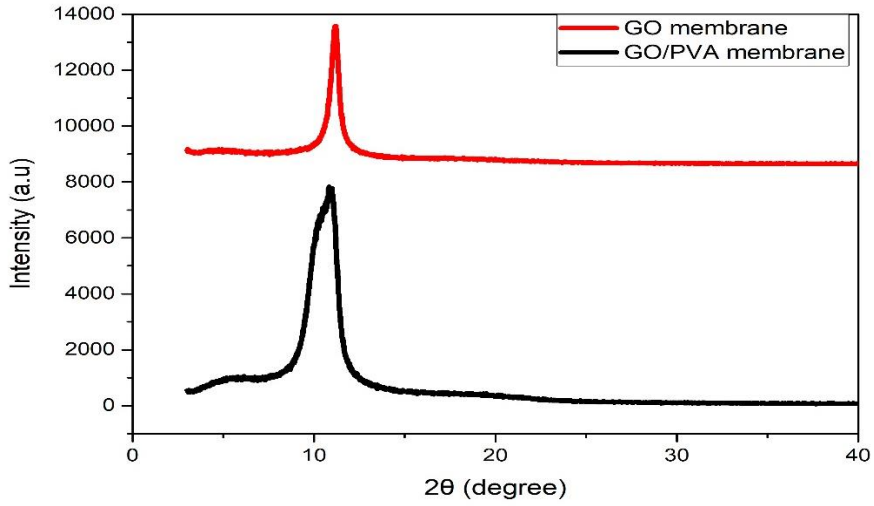

Figure 14: XRD patterns of GO and GO/PVA membranes.

3.5 Filtration of Pharmaceuticals

3.5.1 With GO/PVDF membranes

GO/PVDF membranes exhibit selective permeability toward pharmaceutical compounds depending on their molecular properties, particularly charge and aromaticity. In this study, citalopram, a weakly basic aromatic pharmaceutical, showed a decrease in absorbance intensity after filtration through the GO/PVDF membrane which indicated partial retention of the pharmaceutical on the membrane. This behaviour can be attributed to positive charge acquired by citalopram through protonation of its protonation of its amine group in aqueous solution. Therefore,

electrostatic attraction occurred between negatively charged functional groups on GO, such as carboxylates (-COO^-), and positively charged citalopram molecule.

The results presented in Figure 15 show the UV–Vis spectra of citalopram before and after filtration which indicated a decrease in absorbance from ≈0.37 for the unfiltered sample to 0.27 for the filtered sample. This corresponds to an estimated retention of about 40% of citalopram by the GO/PVDF membrane.

In accordance with the Beer–Lambert law, $A = \varepsilon cl$. Absorbance is directly proportional to the concentration of the absorbing species in solution. Hence, the observed decrease in absorbance at the peak indicates a reduction in citalopram concentration after filtration. This suggests that a portion of the pharmaceutical compound was retained by the GO/PVDF membrane during the filtration process.

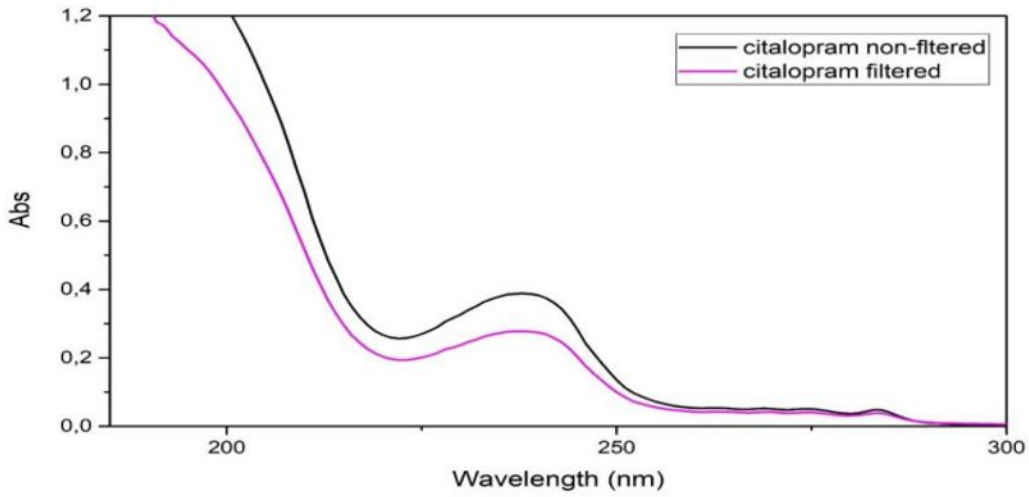

Figure 15: UV-Vis spectra of citalopram before and after filtration through the GO/PVDF membrane.

Correspondingly, in Figure 16 and 17, UV-Vis spectra amisulpride and metoprolol respectively. Both compounds are weakly basic aromatic pharmaceuticals and are positively charged in aqueous solution. Similar to Citalopram, electrostatic attraction occurred between their protonated functional groups and the negatively charged oxygen-containing groups on the GO surface, resulting in a slight decrease in their concentration after filtration.

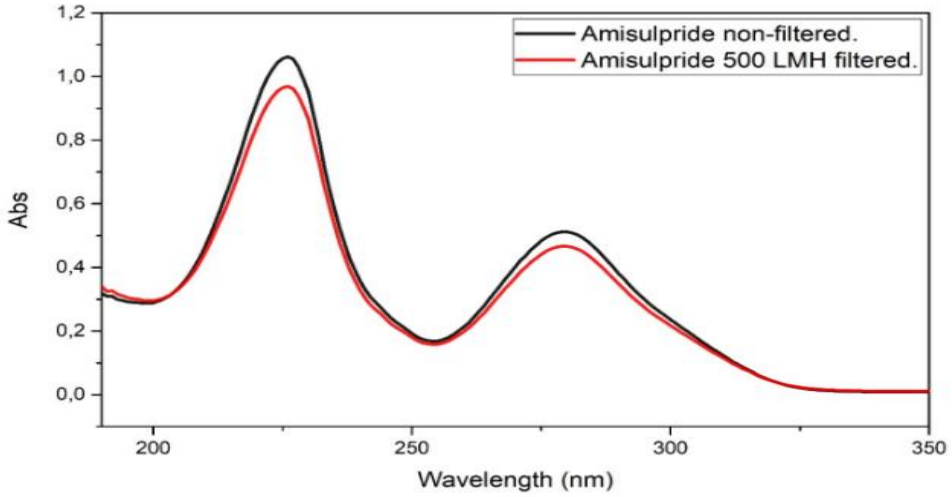

Figure 16: UV-Vis spectra of Amisulpride before and after filtration through the GO/PVDF membrane.

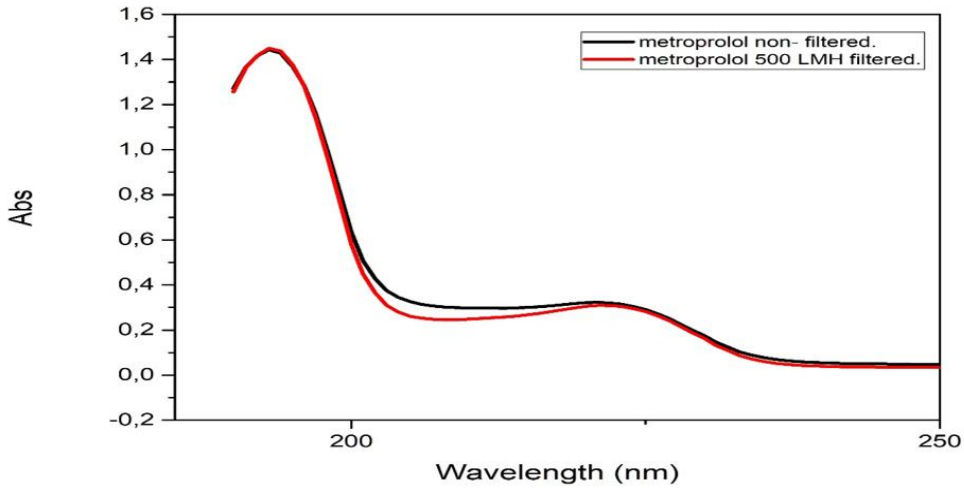

Figure 17: UV-Vis spectra of Metoprolol before and after filtration through the GO/PVDF membrane.

In contrast Figure 18 presents the UV-Vis spectra of diclofenac, an acidic aromatic pharmaceutical which showed negligible retention by the GO/PVDF membrane. This indicates that diclofenac is deprotonated and carries negative charge at neutral pH. Unlike basic pharmaceuticals, it experiences electrostatic repulsion from the

negatively charged GO surface.

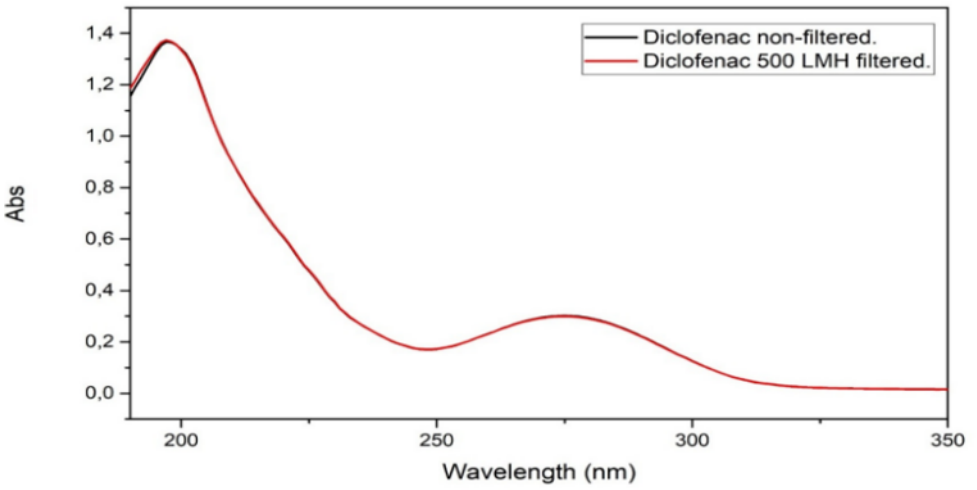

Figure 18: UV-Vis spectra of Diclofenac before and after filtration through the GO/PVDF membrane.

The UV-Vis spectra of carbamazepine shown in Figure 19 exhibits no detectable retention or adsorption on the GO/PVDF membrane after filtration. Carbamazepine is a neutral compound and remains uncharged at neutral pH.

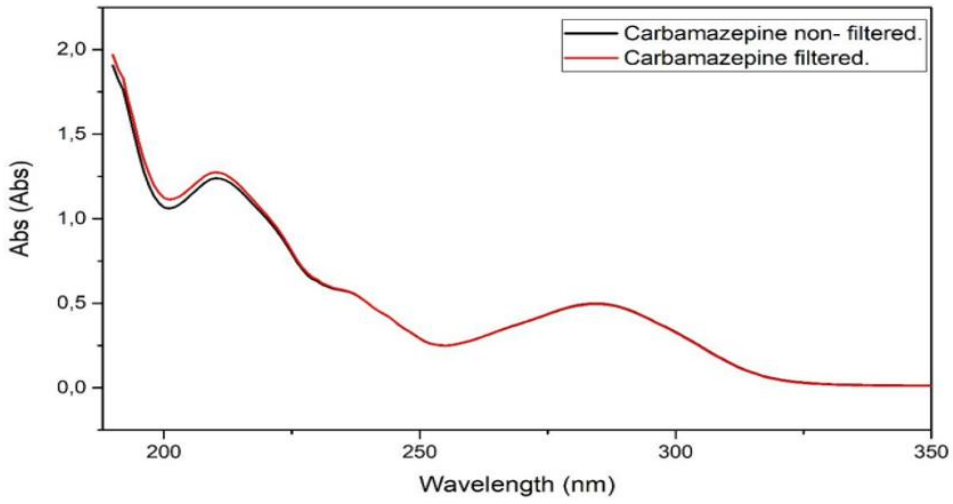

Figure 19: UV-Vis spectra of carbamazepine before and after filtration through the GO/PVDF membrane.

Overall, these results demonstrate that GO/PVDF membrane exhibits selective interactions with pharmaceutical compounds. Stronger adsorption is observed for cationic species, such as protonated citalopram, due to electrostatic attraction. In contrast, acidic or neutral compounds, such as diclofenac and carbamazepine, show minimal interaction. This selective behaviour highlights the critical roles of molecular

charge, protonation state, and electrostatic interactions between GO and pharmaceutical molecules.

The chemical structures of the studied pharmaceutical are shown in Figure 20.

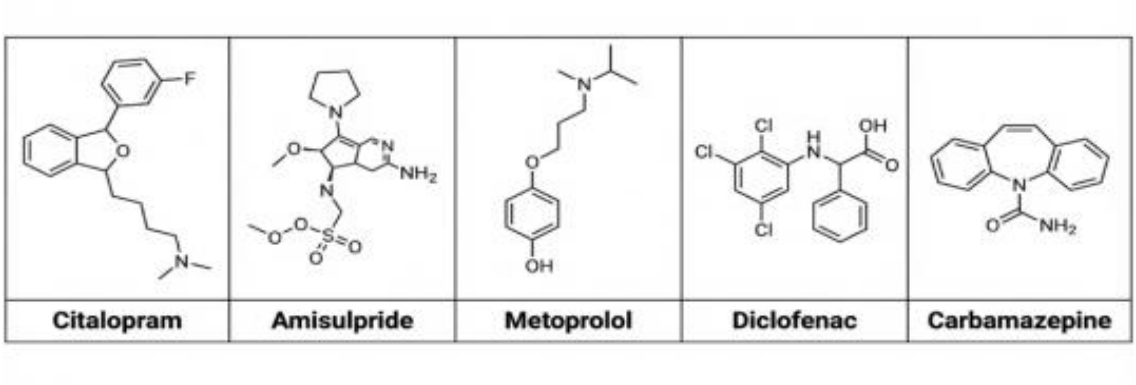

Figure 20: Chemical structures of the pharmaceuticals.

3.5.2 With GO/PVA Membranes

The incorporation of PVA into the GO membrane significantly contradicts the removal behaviour of the investigated pharmaceuticals compared to the GO membrane as seen in the following figures below.

In figure 21, carbamazepine indicates a noticeable decrease in its concentration after filtration through GO/PVA membrane which indicates improved retention of the drug molecule.

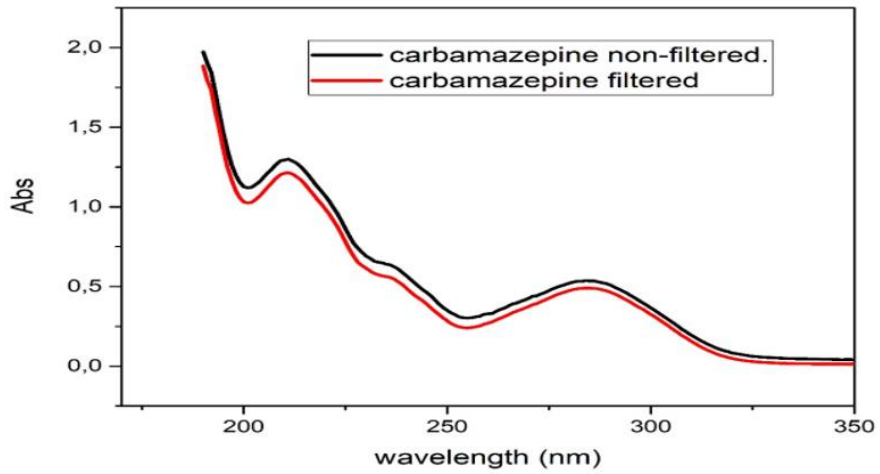

Figure 21: UV-Vis spectra of carbamazepine before and after filtration through the GO/PVA membrane.

However, Figure 22 reveals a negligible decrease in diclofenac concentration which implies minimal interaction of the drug molecule with the modified membrane.

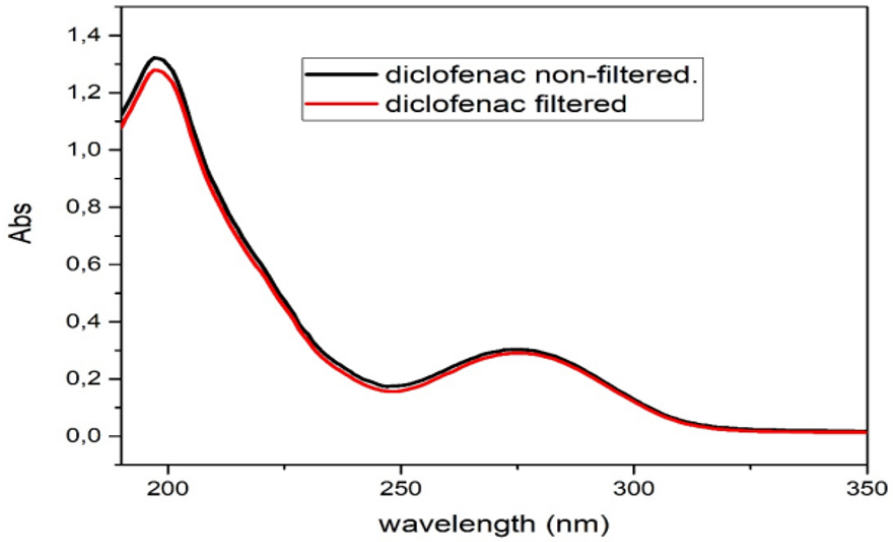

Figure 22: UV-Vis spectra of Diclofenac before and after filtration through GO/PVA membrane.

In contrast, Figure 23 depicts that the concentration of Citalopram remained unchanged after filtration through the GO/PVA membrane.

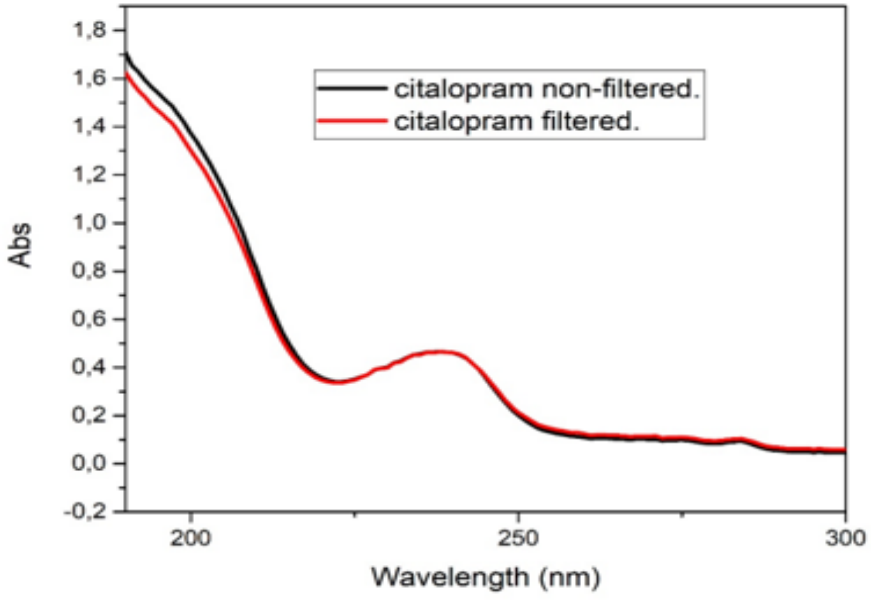

Figure 23: UV-Vis spectra of citalopram before and after filtration through GO/PVA membrane.

The observed results suggest that the incorporation of PVA alters the separation mechanism of the membrane.

3.6 MEMBRANES PERFORMANCE TEST USING FO TECHNIQUE

3.6.1 GO/PVDF Membrane

The performance of the membranes was evaluated using FO technique. In Figure 24, the GO/PVDF membrane was used as the separation membrane. It showed increase in the conductivity measurement of the feed solution for every 15 minutes interval. There is no significant increase in the volume of the draw solution after 1 hour of the experiment but there is high difference in the conductivity measurement for every 15 minutes interval. It exhibited a sharp increase in feed solution conductivity during the first 15 minutes, which indicated substantial reverse salt flux from the draw solution to the feed side. The conductivity then decreased temporarily at 30 minutes before gradually increasing again until the end of the experiment.

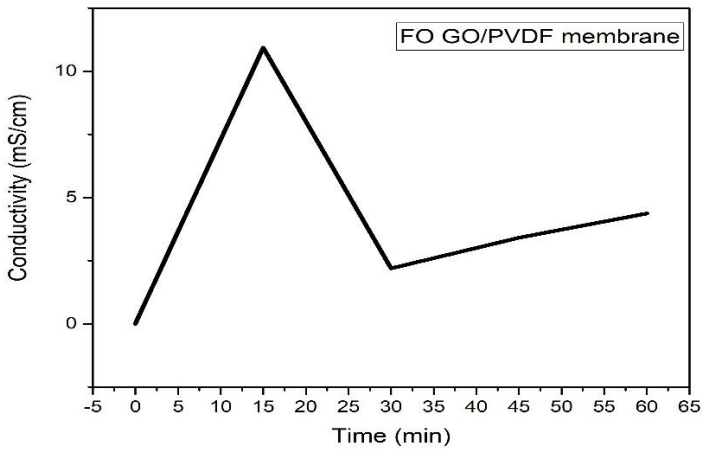

Figure 24: Graphical representation of the FO experiment using GO membrane.

3.6.2 GO/PVA Membrane

In contrary, Figure 25 demonstrates the result of the FO when GO was incorporated with a polymer, PVA. The results showed that the volume of water in the draw solution remained nearly constant during the first 15 minutes and then gradually increased over the course of the experiment which indicated water transport through the membrane. In addition, the salt concentration in the feed solution increased linearly at 15-minute intervals throughout the 2-hour experimental period. The membrane exhibited a gradual increase in both feed solution conductivity and draw solution volume, thereby suggesting reverse salt flux and successful water transport across the membrane.

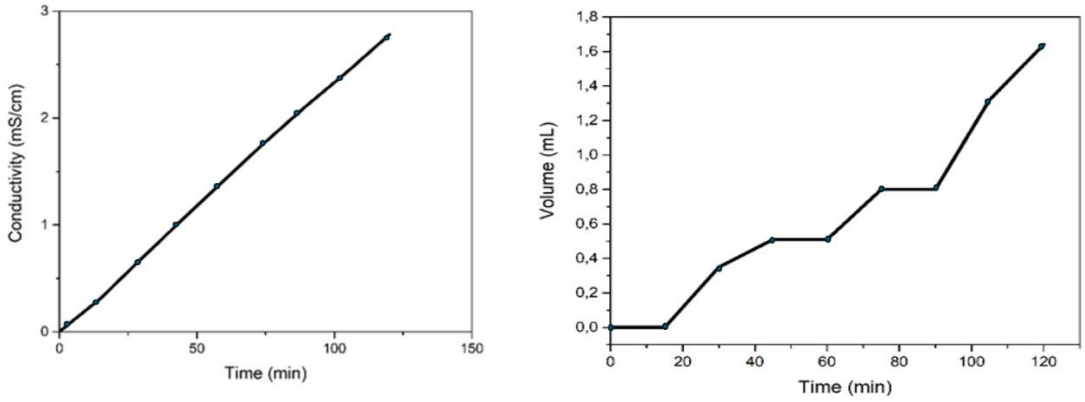

A B

Figures 25: Graphical Representation of the FO experiment using GO/PVA Membrane.

Comparably, GO/PVA membrane exhibited better water flux and lower salt leakage which confirms improved membrane selectivity and performance. This improvement may be attributed to the hydrophilic nature of PVA, which enhanced membrane wettability, permeability, and structural stability of the membrane during the FO process.

4 CONCLUSION

This thesis demonstrated the application of GO-based membranes for the removal of pharmaceutical contaminants from aqueous solutions, and the change in structural and mechanical strength of the membrane when intercalated with a polymer. GO and GO membranes were successfully synthesized using a modified Hummers' and vacuum filtration methods respectively.

The characterization techniques of the materials were done using UV-Vis spectroscopy, Raman spectroscopy, XRD diffractometer, and FTIR spectrometer. These techniques confirmed the successful synthesis of GO and the formation of GO-based membranes. Furthermore, the analysis revealed changes in the properties of the membrane including an increase in the interlayer spacing of GO compared to graphite. These features played a key role in governing membrane–solute interactions.

Filtration experiments were analysed using a syringe filtration system and FO. The syringe filtration results demonstrated that membrane performance depended on the molecular charge, protonation and electrostatic attraction between the membrane surface and pharmaceutical compounds. Positively charged pharmaceuticals exhibited higher interaction with the GO/PVDF membrane, while neutral and negatively charged compounds showed lower retention. The incorporation of PVA modified the membrane surface properties and separation behaviour, leading to altered interaction patterns between the membrane and the pharmaceutical compounds.

FO experiments further revealed that the GO/PVA membrane exhibited improved water transport and reduced reverse salt flux compared to the pristine GO/PVDF membrane. These results indicate that membrane modification enhanced its selectivity and structural stability, resulting to improved overall performance of the membrane.

Overall, the findings of this study demonstrate that GO-based membranes have significant potential for pharmaceutical removal from its aqueous solution. The performance of the membranes is strongly influenced by both membrane composition and the chemical properties of the target contaminants. The

incorporation of a polymer is shown to be an effective strategy for improving membrane functionality, particularly in FO applications.

Future work should focus on optimizing membrane fabrication parameters, improving long-term stability, and evaluating performance under real wastewater conditions to further evaluate practical applicability.

References

1. Kümmerer, K. (2009). The presence of pharmaceuticals in the environment due to human use – Present knowledge and future challenges. Journal of Environmental Management, 90(8), 2354–2366.
2. Son, H.-J., & Jang, S.-H. (2011). Occurrence of residual pharmaceuticals and fate, residue and toxic effect in drinking water resources. Journal of Korean Society of Environmental Engineers, 33(6), 453–479.
3. Heberer, T. (2002). Occurrence, fate, and removal of pharmaceutical residues in the aquatic environment: A review of recent research data. Toxicology Letters, 131(1–2), 5–17.
4. Brodie, B. C. (1859). On the atomic weight of graphite. Philosophical Transactions of the Royal Society of London, 149, 249–259.
5. Staudenmaier, L. (1898). Graphite oxide study. Berichte der Deutschen Chemischen Gesellschaft.
6. Hummers, W. S., & Offeman, R. E. (1958). Preparation of graphitic oxide. Journal of the American Chemical Society, 80, 1339–1339.
7. Croft, R. C. (1960). Lamellar compounds of graphite. Quarterly Reviews, Chemical Society, 14, 1–45.
8. Schäfer, A. I., Fane, A. G., & Waite, T. D. (2005). Nanofiltration: Principles and applications. Elsevier.
9. Sun, P., Wang, Y., Liu, H., Wang, K., Wu, D., Xu, Z., & Zhu, H. (2014). Structure evolution of graphene oxide during thermally driven phase transformation: Is the oxygen content really preserved? PLoS ONE, 9, 1–8.
10. Lerf, A., He, H., Forster, M., & Klinowski, J. (1998). Structure of graphite oxide revisited. The Journal of Physical Chemistry B, 102, 4477–4482.
11. Li, D., & Kaner, R. B. (2008). Graphene-based materials. Science, 320, 1170–1171.
12. Gao, W., Alemany, L. B., Ci, L., & Ajayan, P. M. (2009). New insights into the structure and reduction of graphite oxide. Nature Chemistry, 1, 403–408.
13. Park, S., & Ruoff, R. S. (2009). Chemical methods for the production of graphenes. Nature Nanotechnology, 4, 217–224.

14. Rao, C. N. R., Sood, A. K., Subrahmanyam, K. S., & Govindaraj, A. (2009). Graphene: The new two-dimensional nanomaterial. Angewandte Chemie International Edition, 48, 7752–7777.
15. Allen, M. J., Tung, V. C., & Kaner, R. B. (2010). Honeycomb carbon: A review of graphene. Chemical Reviews, 110, 132–145.
16. Compton, O. C., & Nguyen, S. T. (2010). Graphene oxide, highly reduced graphene oxide, and graphene: Versatile building blocks for carbon-based materials. Small, 6, 711–723.
17. Eda, G., & Chhowalla, M. (2010). Chemically derived graphene oxide: Towards large-area thin-film electronics and optoelectronics. Advanced Materials, 22, 2392–2415.
18. Liu, G., Jin, W., & Xu, N. (2015). Graphene-based membranes. *Chemical Society Reviews, 44*(15), 5016–5030.
19. Perreault, F., De Faria, A. F., Nejati, S., & Elimelech, M. (2015). Antimicrobial properties of graphene oxide nanosheets: Why size matters. *ACS Nano, 9*(7), 7226–7236.
20. Liu, G., Jin, W., & Xu, N. (2015). Graphene-based membranes. *Chemical Society Reviews, 44*(15), 5016–5030.
21. Joshi, R. K., Carbone, P., Wang, F. C., Kravets, V. G., Su, Y., Grigorieva, I. V., Wu, H. A., Geim, A. K., & Nair, R. R. (2014). Precise and ultrafast molecular sieving through graphene oxide membranes. *Science, 343*(6172), 752–754.
22. Mulder, M. (1996). *Basic principles of membrane technology* (2nd ed.). Springer.
23. Fent, K., Weston, A., & Caminada, D. (2006). Ecotoxicology of human pharmaceuticals. Aquatic Toxicology, 76(2), 122–159.
24. Karan, S., Jiang, Z., & Livingston, A. G. (2015). Sub-10 nm polyamide nanofilms with ultrafast solvent transport for molecular separation. Science, 348, 1347–1351.
25. Wang, Y., He, Z., Gupta, K. M., Shi, Q., & Lu, R. (2017). Molecular dynamics study on water desalination through functionalized nanoporous graphene. Carbon, 116, 120–127.
26. Jain, T., et al. (2015). Heterogeneous sub-continuum ionic transport in statistically isolated graphene nanopores. Nature Nanotechnology, 10, 1053–1057.

27. Surwade, S. P., et al. (2015). Water desalination using nanoporous single layer graphene. Nature Nanotechnology, 10, 459–464.
28. O'Hern, S. C., et al. (2014). Selective ionic transport through tunable subnanometer pores in single-layer graphene membranes. Nano Letters, 14, 1234–1241.
29. O'Hern, S. C., et al. (2012). Selective molecular transport through intrinsic defects in a single layer of CVD graphene. ACS Nano, 6, 10130–10138.
30. Koenig, S. P., Wang, L., Pellegrino, J., & Bunch, J. S. (2012). Selective molecular sieving through porous graphene. Nature Nanotechnology, 7, 728–732.
31. Wang, E. N., & Karnik, R. (2012). Graphene cleans up water. Nature Nanotechnology, 7, 552–554.
32. Cohen-Tanugi, D., & Grossman, J. C. (2012). Water desalination across nanoporous graphene. Nano Letters, 12, 3602–3608.
33. Wang, Z., & Mi, B. (2017). Environmental applications of 2D molybdenum disulfide (MoS_2) nanosheets. Environmental Science & Technology, 51, 8229–8244.
34. Wang, Z., et al. (2017). Understanding the aqueous stability and filtration capability of MoS_2 membranes. Nano Letters, 17, 7289–7298.
35. Abraham, J., et al. (2017). Tuneable sieving of ions using graphene oxide membranes. Nature Nanotechnology, 12, 546–550.
36. Li, H., et al. (2013). Ultrathin, molecular-sieving graphene oxide membranes for selective hydrogen separation. Science, 342, 95–98.
37. Joshi, R. K., Carbone, P., Wang, F. C., Kravets, V. G., Su, Y., Grigorieva, I. V., Wu, H. A., Geim, A. K., & Nair, R. R. (2014). Precise and ultrafast molecular sieving through graphene oxide membranes. *Science, 343*(6172), 752–754.
38. Nair, R. R., Wu, H. A., Jayaram, P. N., Grigorieva, I. V., & Geim, A. K. (2012). Unimpeded permeation of water through helium-leak-tight graphene-based membranes. Science, 335, 442–444.
39. Homaeigohar, S., & Elbahri, M. (2017). Graphene membranes for water desalination. NPG Asia Materials, 9, e427.
40. Werber, J. R., Osuji, C. O., & Elimelech, M. (2016). Materials for next generation desalination and water purification membranes. Nature Reviews Materials, 1, 1–15.

41. Bera, S., et al. (2023). 2D-nanofiller-based polymer nanocomposites for capacitive energy storage applications. Small Science, 3, 2300016.
42. Sonker, M., et al. (2022). Ammonia as an alternative fuel for vehicular applications: Paving the way for adsorbed ammonia and direct ammonia fuel cells. Journal of Cleaner Production, 376, 133960.
43. Alkhouzaam, A., & Qiblawey, H. (2021). Functional GO-based membranes for water treatment and desalination: Fabrication methods, performance and advantages. Chemosphere, 274, 129853.
44. Yang, Q., et al. (2017). Ultrathin graphene-based membrane with precise molecular sieving and ultrafast solvent permeation. Nature Materials, 16, 1198–1202.
45. Huang, H., Mao, Y., Ying, Y., Liu, Y., Sun, L., & Peng, X. (2013). Salt concentration, pH and pressure-controlled separation of small molecules through lamellar graphene oxide membranes. Chemical Communications, 49, 5963–5965.
46. Cao, Y., Xiong, Z., Xia, F., Franks, G. V., Zu, L., Wang, X., Hora, Y., Mudie, S., He, Z., Qu, L., Xing, Y., & Li, D. (2022). Advanced Functional Materials, 32, 2201535.
47. Liu, M.-L., Guo, J.-L., Japip, S., Jia, T.-Z., Shao, D.-D., Zhang, S., Li, W.-J., Wang, J., Cao, X.-L., & Sun, S.-P. (2019). Journal of Materials Chemistry A, 7, 3170–3178.
48. Xu, F., Song, Y., Wei, M., & Wang, Y. (2018). The Journal of Physical Chemistry C, 122, 15772–15779.
49. Tang, S., Zhang, L., Peng, Y., Liu, J., Zhang, X., & Zhang, Z. (2019). Corrigendum to Fenton cleaning strategy for ceramic membrane fouling in wastewater treatment. Journal of Environmental Sciences, 86, 236.
50. Kumar, C. M., Roshni, M., & Vasanth, D. (2019). Treatment of aqueous bacterial solution using ceramic membrane prepared from cheaper clays: A detailed investigation of fouling and cleaning. Journal of Water Process Engineering, 29, 100797.
52. Wen, Y., Yuan, J., Ma, X., Wang, S., & Liu, Y. (2019). Polymeric nanocomposite membranes for water treatment: A review. Environmental Chemistry Letters, 17, 1539–1551.
53. Wankat, P. C. (2006). Separation process engineering. Pearson Education.

54.Dreyer, D. R., Park, S., Bielawski, C. W., & Ruoff, R. S. (2010). The chemistry of graphene oxide. Chemical Society Reviews, 39, 228–240.

55. Abraham, J., Vasu, K. S., Williams, C. D., Gopinadhan, K., Su, Y., Cherian, C. T., Dix, J., Prestat, E., Haigh, S. J., & Grigorieva, I. V. (2017). Tunable sieving of ions using graphene oxide membranes. Nature Nanotechnology, 12, 546–550.

56. Joshi, R. K., Carbone, P., Wang, F. C., Kravets, V. G., Su, Y., Grigorieva, I. V., Wu, H. A., Geim, A. K., & Nair, R. R. (2014). Precise and ultrafast molecular sieving through graphene oxide membranes. Science, 343, 752–754.

57. Huang, H., Mao, Y., Ying, Y., Liu, Y., Sun, L., & Peng, X. (2013). Salt concentration, pH and pressure controlled separation of small molecules through lamellar graphene oxide membranes. Chemical Communications, 49, 5963.

58. Yu, P., Xiong, Z., Zhan, H., Xie, K., Zhong, Y. L., Simon, G. P., & Li, D. (2019). Electrochemically-derived graphene oxide membranes with high stability and superior ionic sieving. Chemical Communications, 55, 4075–4078.

59. Tian, L., Zhou, P., Graham, N., Li, G., & Yu, W. (2023). Long-term operation and biofouling of graphene oxide membrane in practical water treatment: Insights from performance and biofilm characteristics. Journal of Membrane Science, 680, 121761.

60. Hong, S., Constans, C., Martins, M. V. S., Seow, Y. C., Carrió, J. A. G., & Garaj, S. (2017). Scalable graphene-based membranes for ionic sieving with ultrahigh charge selectivity. Nano Letters, 17, 728–732.

61. Talyzin, A. V., Hausmaninger, T., You, S., & Szabó, T. (2014). The structure of graphene oxide membranes in liquid water, ethanol and water–ethanol mixtures. Nanoscale, 6, 272–281.

62. Park, S., Lee, K.-S., Bozoklu, G., Cai, W., Nguyen, S. T., & Ruoff, R. S. (2008). Graphene oxide papers modified by divalent ions—Enhancing mechanical properties via chemical cross-linking. ACS Nano, 2, 572–578.

63. Liu, T., Yang, B., Graham, N., Yu, W., & Sun, K. (2017). Trivalent metal cation cross-linked graphene oxide membranes for NOM removal in water treatment. Journal of Membrane Science, 542, 31–40.

64. Huang, L., Zhang, M., Li, C., & Shi, G. (2015). Graphene-based membranes for molecular separation. The Journal of Physical Chemistry Letters, 6, 2806–2815.

65. Han, Y., Xu, Z., & Gao, C. (2013). Ultrathin graphene nanofiltration membrane for water purification. Advanced Functional Materials, 23, 3693–3700.

66. Huang, L., Chen, J., Gao, T., Zhang, M., Li, Y., Dai, L., Qu, L., & Shi, G. (2016). Reduced graphene oxide membranes for ultrafast organic solvent nanofiltration. Advanced Materials, 28, 8669–8674.

67. Huang, H. H., Joshi, R. K., De Silva, K. K. H., Badam, R., & Yoshimura, M. (2019). Fabrication of reduced graphene oxide membranes for water desalination. Journal of Membrane Science, 572, 12–19.

68. Zhang, Q., Qian, X., Thebo, K. H., Cheng, H.-M., & Ren, W. (2018). Controlling reduction degree of graphene oxide membranes for improved water permeance. Science Bulletin, 63, 788–794.

69. Yang, E., Ham, M.-H., Park, H. B., Kim, C.-M., Song, J.-H., & Kim, I. S. (2018). Tunable semi-permeability of graphene-based membranes by adjusting reduction degree of laminar graphene oxide layer. Journal of Membrane Science, 547, 73–79.

70. Xi, Y.-H., Liu, Z., Liao, Q.-C., Xie, R., Ju, X.-J., Wang, W., Faraj, Y., & Chu, L.-Y. (2018). Effect of oxidized-group-supported lamellar distance on stability of graphene-based membranes in aqueous solutions. Industrial & Engineering Chemistry Research, 57, 9439–9447.

71. Malik, M., Chan, K. H., & Azimi, G. (2021). Quantification of nickel, cobalt, and manganese concentration using ultraviolet-visible spectroscopy. RSC Advances, 11, 28014–28028.

72. Moseley, H. H. G. J., & Darwin, C. G. (1913). On the reflexion of the X-rays. The London, Edinburgh, and Dublin Philosophical Magazine and Journal of Science, 26(151), 210–232.

73. Cuong, T. V., Pham, V. H., Tran, Q. T., Hahn, S. H., Chung, J. S., Shin, E. W., & Kim, E. J. (2010).
Photoluminescence and Raman studies of graphene thin films prepared by reduction of graphene oxide. Materials Letters, 64(3), 399–401.

74. J. I. Paredes, S. Villar-Rodil, P. Solís-Fernández, A. Martínez-Alonso, J. M. D. Tascón, *Langmuir* 2009, 25, 5957.

75. M. F. Islam, E. Rojas, D. M. Bergey, A. T. Johnson, A. G. Yodh, *Nano Lett.* 2003, 3, 269.

76. Moseley, H. G. J. (1913). The high-frequency spectra of the elements. The London, Edinburgh and Dublin Philosophical Magazine and Journal of Science, 26, 1024–1034.

77. Tuinstra, F., & Koenig, J. L. (1970). Raman spectrum of graphite. The Journal of Chemical Physics, 53(3), 1126–1130.

78. Pimenta, M. A., Dresselhaus, G., Dresselhaus, M. S., Cancado, L. G., & Jorio, A., & Saito, R. (2007). Studying disorder in graphite-based systems by Raman spectroscopy. *Physical Chemistry Chemical Physics, 9*, 1276–1291.

79. Stankovich, S., et al. (2007). Synthesis of graphene-based nanosheets via chemical reduction of exfoliated graphite oxide. *Carbon, 45*, 1558–1565.

80 Zhang, Y., Hao, H., & Wang, L. (2016). Effect of morphology and defect density on electron transfer of electrochemically reduced graphene oxide. *Applied Surface Science, 390*, 385–392.

81. Stankovich, S., Piner, R. D., Nguyen, S. T., & Ruoff, R. S. (2006). Synthesis and exfoliation of isocyanate-treated graphene oxide nanoplatelets. Carbon, 44(15), 3342–3347.

82. Golsheikh, A. M., Huang, N. M., Lim, H. N., Zakaria, R. & Yin, C. Y. One-step electrodeposition synthesis of silver-nanoparticle-decorated graphene on indium-tin-oxide for enzymeless hydrogen peroxide detection. *Carbon* 62, 405–412 (2013).